

000 001 FAIR GRAPH MACHINE LEARNING UNDER ADVERSAR- 002 IAL MISSINGNESS PROCESSES 003 004

005 **Anonymous authors**
006 Paper under double-blind review

007 008 ABSTRACT 009

011 Graph Neural Networks (GNNs) have achieved state-of-the-art results in many rel-
012 evant tasks where decisions might disproportionately impact specific communities.
013 However, existing work on fair GNNs often assumes that either sensitive attributes
014 are fully observed or they are missing completely at random. We show that an
015 adversarial missingness process can inadvertently disguise a fair model through the
016 imputation, leading the model to overestimate the fairness of its predictions. We
017 address this challenge by proposing Better Fair than Sorry (BFtS), a fair missing
018 data imputation model for sensitive attributes. The key principle behind BFtS is
019 that imputations should approximate the worst-case scenario for fairness—i.e.,
020 when optimizing fairness is the hardest. We implement this idea using a 3-player
021 adversarial scheme where two adversaries collaborate against a GNN classifier,
022 and the classifier minimizes the maximum bias. Experiments using synthetic and
023 real datasets show that BFtS often achieves a better fairness \times accuracy trade-off
024 than existing alternatives under an adversarial missingness process.

025 026 1 INTRODUCTION 027

029 With the increasing popularity of machine learning in high-stakes decision-making, it has become a
030 consensus that these models carry implicit biases that should be addressed to improve the fairness
031 of algorithmic decisions (Ghallab, 2019). The disparate treatment of such models towards African
032 Americans and women has been illustrated in the well-documented COMPAS (Angwin et al., 2022)
033 and Apple credit card (Vigdor, 2019) cases, respectively. While there has been extensive research on
034 fair ML, the proposed solutions have mostly disregarded important challenges that arise in real-world
035 settings. For instance, in many applications, data can be naturally modeled as graphs (or networks),
036 representing different objects, their relationships, and attributes, instead of as sequences or images.
037 Moreover, fair ML is also prone to missing data (Little & Rubin, 2019). This is particularly critical
038 because fair algorithms often require knowledge of sensitive attributes that are more likely to be
039 missing due to biases in the collection process or privacy concerns. For instance, census and health
040 surveys exhibit missingness correlated with gender, age, and race (O’Hare & O’Hare, 2019; Weber
041 et al., 2021). Networked data, such as disease transmission studies, face similar issues (Ghani et al.,
042 1998). As a consequence, fair ML methods often rely on missing data imputation, which can introduce
043 errors that compromise fairness (Mansoor et al., 2022; Jeong et al., 2022).

044 This work investigates the impact of adversarial sensitive value missingness processes on fairness,
045 where the pattern of missing sensitive data is structured to obscure true disparities. If the predictions
046 from the imputation method fail to capture the true distribution of a sensitive attribute, any fairness-
047 aware model trained on the imputed data is prone to inheriting the underlying true bias. More
048 specifically, a key challenge arises when an adversarial missingness process makes the imputed
049 dataset appear to be fair. In graphs, an adversary can exploit the graph structure to manipulate the
050 imputed values and, as a consequence, the fairness-aware model. Prior work on the fairness of graph
051 machine learning assumes sensitive values are Missing Completely At Random (MCAR). However,
052 this assumption rarely holds in practice (O’Hare & O’Hare, 2019; Weber et al., 2021; Ghani et al.,
053 1998; Jeong et al., 2022). Luh (2022) and Fukuchi et al. (2020) provide motivational examples of how
fairness can be manipulated by adversarial data collection. Methods that overlook the adversarial
missingness process risk producing misleading fairness guarantees w.r.t. the complete data.

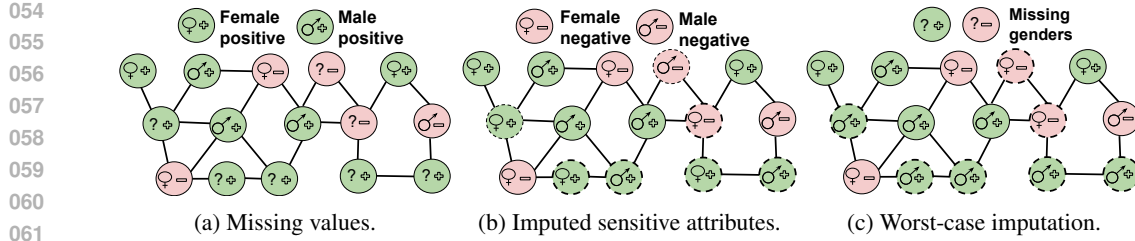


Figure 1: In Fig. (a), a graph machine learning algorithm is applied to decide who receives credit (positive or negative) based on a possibly missing sensitive attribute, gender (and binary only for illustrative purposes). As shown in Fig. (b), traditional missing data imputation does not account for outcomes (positive/negative), and thus, their imputed values can under-represent the bias of the complete dataset—demographic parity (DP) is 0.09 in this example (DP and bias are inversely related). This paper proposes BFtS, an imputation method for graph data that optimizes fairness in the worst-case imputation scenario using adversarial learning, as shown in Fig. (c), where DP is 0.47.

Figure 1 motivates our problem setting using a toy example. A machine learning algorithm is applied to decide whether individuals should or should not receive credit. Figure 1a shows both the gender and outcome for each individual. The genders of some samples are unknown in Figure 1a, and the demographic parity (ΔDP) considering only the observed values is 0.25 (ΔDP is a bias metric described in Section 5). We illustrate how different missing data imputations affect the fairness of credit decisions in Figures 1b and 1c. A straightforward imputation is demonstrated in Figure 1b, where the gender of the majority of neighbors is assigned to the missing attribute, resulting in a best-case scenario in terms of fairness with a ΔDP of 0.09. However, in the worst-case scenario, shown in Figure 1c, ΔDP is 0.47. If an adversarial missingness process can induce the imputation model to generate the imputation from Figure 1b but the complete data is Figure 1c, a fair model trained on the imputed data will still be biased w.r.t. the complete data.

To counter an adversarial missingness process for sensitive values on graphs, we propose Better Fair than Sorry (BFtS), a 3-player adversarial learning framework for missing sensitive value imputation based on Graph Neural Networks (GNNs). Our experiments show that BFtS achieves a better accuracy \times fairness trade-off than existing approaches, especially under adversarial missing sensitive values.

We summarize our contributions as follows: (1) We investigate theoretically and empirically the potential of an adversarial missingness process to bias a fair GNN; (2) We propose Better Fair than Sorry (BFtS), a novel 3-player adversarial learning framework for the imputation of missing sensitive data that produces worst-case imputed values for fair GNNs and is effective under adversarial missingness processes and even when sensitive attribute information is completely unavailable; and (3) We show empirically that BFtS achieves a better fairness \times accuracy trade-off than the baselines.

1.1 RELATED WORK

Fairness in graph machine learning. Our work is focused on group fairness Pessach & Shmueli (2022); Dong et al. (2023). Existing work can be grouped into pre-processing, extended objectives, and adversarial learning. Pre-processing methods such as FairOT, FairDrop, FairSIN, EDITS, and Graphair remove bias from the graph before training (Laclau et al., 2021; Spinelli et al., 2021; Yang et al., 2024; Dong et al., 2022; Ling et al., 2023). Objective-based methods—including Fairwalk, Crosswalk, Debayes, MONET, NIFTY, FairVGNN, PFR-AX, FairSAD, and FairGAE—modify GNN losses to learn fair representations (Rahman et al., 2019; Khajehnejad et al., 2022; Buyl & De Bie, 2020; Palowitch & Perozzi, 2019; Agarwal et al., 2021; Wang et al., 2022; Merchant & Castillo, 2023; Zhu et al., 2024; Fan et al., 2021). Adversarial methods such as CFC, FLIP, DKGE, and Debias jointly train GNNs with adversaries for fair prediction (Bose & Hamilton, 2019; Masrour et al., 2020; Arduini et al., 2020; Zhang et al., 2018). All these require fully observed sensitive attributes.

Missing Data Imputation and fairness. Missing data can be imputed using unconditional mean, reconstruction, preferential attachment, autoencoders, etc. (Donders et al., 2006; Pereira et al., 2020; Huisman, 2009). The traditional procedure for handling missing data is independent imputation—i.e., to first impute the missing values and then solve the task (Rossi et al., 2021; Buck, 1960). SAT is a

108 matching-based GNN for graphs with missing attributes (Chen et al., 2020), but it does not account
 109 for fairness. Training a classifier from imputed data can amplify the bias of a machine learning model,
 110 as discussed in (Subramonian et al., 2022; Zhang & Long, 2021; Feng et al., 2023; Guha et al., 2024;
 111 Martínez-Plumed et al., 2019; Fricke, 2020; Mansoor et al., 2022). Some studies try to generate fair
 112 feature imputations (Subramonian et al., 2022; Feng et al., 2023; Jeong et al., 2022; Zhang & Long,
 113 2022). However, as the approaches discussed earlier, these methods do not consider missing sensitive
 114 information and require full knowledge of the sensitive attributes for fairness intervention.

115 **Fairness with missing sensitive attributes.** One extreme assumption is the complete unavailability
 116 of sensitive information. For example, Hashimoto et al. (2018) considers the worst-case distribution
 117 over group sizes, Lahoti et al. (2020) reweights training samples adversarially, Chai & Wang (2022)
 118 minimizes a top- k average loss, and Zhao et al. (2022) reduces correlation between predictions and
 119 features associated with sensitive attributes. Other approaches include class re-balancing (Yan et al.,
 120 2020) and soft labels from an overfitted teacher (Chai et al., 2022). In practice, partial sensitive
 121 information is often available and improves fairness (Chai & Wang, 2022), but these models fail to
 122 leverage it. FairGNN (Dai & Wang, 2021) assumes limited sensitive data and imputes missing values
 123 independently, FairAC (Guo et al., 2023) uses only observed attributes without imputation, and RNF
 124 (Du et al., 2021) generates proxy annotations using generalized cross-entropy (Zhang & Sabuncu,
 125 2018). Similar to RNF, our approach handles completely or partially missing sensitive information.
 126 BFtS applies a 3-player scheme to minimize the maximum possible bias and outperforms FairGNN
 127 and RNF in terms of fairness \times accuracy. Minimizing the maximum instead of the average risk,
 128 similar to our method, has been shown to achieve better guarantees (Shalev-Shwartz & Wexler, 2016).
 129 A similar minmax approach has been applied to maximize the robustness and accuracy of uncertainty
 130 models (Löfberg, 2003; Lanckriet et al., 2002; Chen et al., 2017; Fauß et al., 2021). In (Nguyen
 131 et al., 2017; Vandenbende et al., 2019), a 3-player adversarial network is proposed to improve the
 132 classification and stability of adversarial learning.

133 **Adversarial attacks on fairness.** Recent work has investigated data poisoning as a means to
 134 adversarially degrade model fairness (Mehrabi et al., 2021; Solans et al., 2020). UnfairTrojan and
 135 TrojFair introduce backdoor attacks specifically aimed at reducing model fairness (Furth et al., 2024;
 136 Zheng et al., 2023). In the context of graph neural networks (GNNs), most adversarial fairness
 137 attacks modify graph topology: Hussain et al. (2022); Zhang et al. (2023) perturb edges, NIFA
 138 injects nodes via uncertainty maximization and homophily enhancement (Luo et al., 2024), and
 139 FATE applies bilevel meta-learning for poisoning (Kang et al., 2023). Thus, prior work has primarily
 140 focused on poisoning, node injection, or structural perturbations, while attacks that compromise
 141 fairness solely by manipulating sensitive-attribute missingness remain unexplored. **In this study, we**
 142 **focus on adversarial missingness rather than data poisoning, as it represents a more practical and**
 143 **plausible threat model in many real-world systems.** Prior work on adversarial missingness in causal
 144 structure learning (Koyuncu et al., 2023; 2024) highlights that when data authenticity is enforced
 145 (e.g., via cryptographically signed sensor records), an adversary cannot modify values or inject
 146 fabricated samples without violating digital-signature constraints. Such tampering would introduce
 147 inconsistencies across logs, backups, and signatures, making it infeasible under standard integrity
 148 guarantees. In contrast, selectively withholding, dropping, or failing to log certain fields does not
 149 break these integrity checks and is indistinguishable from common pipeline failures. Under this threat
 150 model, the adversary is therefore limited to partially concealing existing data and can strategically
 151 choose which sensitive attributes to withhold. This makes adversarial missingness a plausible and
 152 practically relevant mechanism for undermining fairness.

2 PRELIMINARIES

153 Let $\mathcal{G} = (\mathcal{V}, \mathcal{E}, \mathcal{X}, \mathcal{S})$ be an undirected graph where \mathcal{V} is the set of nodes, $\mathcal{E} \subseteq \mathcal{V} \times \mathcal{V}$ is the set of
 154 edges, \mathcal{X} are node attributes, and \mathcal{S} is the set of sensitive attributes. The matrix $A \in \mathbb{R}^{N \times N}$ is the
 155 adjacency matrix of \mathcal{G} where $A_{uv} = 1$ if there is an edge between u and v and $A_{uv} = 0$, otherwise.
 156 We focus on the setting where sensitive attributes might be missing, and only $\mathcal{V}_S \subseteq \mathcal{V}$ nodes include
 157 the information of the sensitive attribute s_v for a node v . The sensitive attribute forms two groups,
 158 which are often called sensitive ($s_v = 1$) and non-sensitive ($s_v = 0$).

159 While our work can be generalized to other fairness-aware tasks, we will focus on binary fair node
 160 classification, where the goal is to learn a classifier f_C to predict node labels $y_v \in \{0, 1\}$ based on a

162 training set $\mathcal{V}_L \subseteq \mathcal{V}$. Without loss of generality, we assume that the class $y = 1$ is the desired one
 163 (e.g., receive credit or bail). Given a classification loss \mathcal{L}_{class} and a **group** fairness loss \mathcal{L}_{bias} , the
 164 goal is to learn the parameters θ_{class} of f_{class} by minimizing their combination:

$$166 \quad \theta_{class}^* = \arg \min_{\theta_{class}} \mathcal{L}_{class} + \alpha \mathcal{L}_{bias}$$

167 where \mathcal{L}_{bias} measures the impact of the sensitive attribute s_v over the predictions from f_{class} and α
 168 is a hyperparameter. The main challenge addressed in this paper is how to handle missing sensitive
 169 attributes. In this scenario, one can apply an independent imputation model $s_v \approx f_{imp}(v)$ before
 170 training the fair classifier. However, the fairness of the resulting classifier will be highly dependent
 171 on the accuracy of f_{imp} , as will be discussed in more detail in the next section.

173 3 INTRODUCING BIAS VIA AN ADVERSARIAL MISSINGNESS PROCESS

176 We investigate the impact of missing sensitive values on fairness in graph machine learning. Datasets
 177 with substantial missingness typically require imputation. In this section, we focus on how the missingness
 178 process (i.e., the process that generates missing values) can lead to (intended or unintended)
 179 biases in a fair model trained using the imputed data, leading fair models to underestimate bias and
 180 remain unfair relative to the complete data.

181 We can describe the missingness process using a threat model. The asset is the graph $\mathcal{G}(\mathcal{V}, \mathcal{E}, \mathcal{X}, \mathcal{S})$,
 182 and the threat is increasing the bias of a node classification model f_{class} applied to \mathcal{G} . The vulnerability
 183 arises because the adversary can select a subset of sensitive attributes $\mathcal{V} \setminus \mathcal{V}_S$ to be missing, thereby
 184 inducing a strategically biased missingness pattern. Our mitigation combines missing-data imputation
 185 and fair node classification to counter such adversarial missingness. The attacker's capabilities and
 186 constraints are described next in the adversarial missingness formulations introduced in this section.

187 The simplest missingness process for sensitive values is *missing completely at random*—i.e., the
 188 probability of a value being missing is independent of the data. However, in practical scenarios,
 189 missing values are rarely random (O'Hare & O'Hare, 2019; Weber et al., 2021; Ghani et al., 1998). We
 190 focus on the particular case where the missingness process is adversarial. We prove that manipulating
 191 the missingness process to induce bias optimally is computationally hard. However, a simple heuristic
 192 can effectively introduce bias to an independent imputation model that simply tries to maximize
 193 imputation accuracy. We formulate the problem for a given number of observed sensitive values k .

194 **Definition 1. Adversarial Missingness Against Fair Classification (AMFC):** Given a graph
 195 $\mathcal{G} = (\mathcal{V}, \mathcal{E})$, select a set of nodes \mathcal{V}_S^* that maximizes the bias of a fair classifier with parameters
 196 θ_{class}^* trained with an imputation model with parameters θ_{imp}^* trained with \mathcal{V}_S :

$$198 \quad \mathcal{V}_S^* = \arg \max_{\mathcal{V}_S \in \mathcal{V}, |\mathcal{V}_S|=k} \mathcal{L}_{bias}(\theta_{class}^*, \mathcal{V})$$

$$199 \quad \text{s.t. } \theta_{class}^* = \arg \min_{\theta_{class}} \mathcal{L}_{class}(\theta_{class}) + \alpha \mathcal{L}_{bias}(\theta_{class}, \theta_{imp}^*, \mathcal{V}_S)$$

$$200 \quad \text{s.t. } \theta_{imp}^* = \arg \min_{\theta_{imp}} \mathcal{L}_{imp}(\theta_{imp}, \mathcal{V}_S)$$

203 where we assume that the adversary can compute the bias $\mathcal{L}_{bias}(\theta_{class}^*, \mathcal{V})$ based on all sensitive
 204 attributes s_v , while the classifier can only estimate its bias based on a combination of nodes \mathcal{V}_S with
 205 observed s_v and imputed values produced with θ_{imp}^* . While AMFC describes the objective of an
 206 idealized adversary, it is impractical due to its associated complexity (tri-level optimization).

207 **Definition 2. Adversarial Missingness against Data Bias (AMADB):** Given a graph $\mathcal{G} = (\mathcal{V}, \mathcal{E})$,
 208 select a set of nodes \mathcal{V}_S^* that minimizes the bias in the labels estimated using an imputation model
 209 with parameters θ_{imp}^* trained with \mathcal{V}_S :

$$210 \quad \mathcal{V}_S^* = \arg \min_{\mathcal{V}_S \in \mathcal{V}, |\mathcal{V}_S|=k} \mathcal{L}_{bias}(\theta_{imp}^*, \mathcal{V}_S, \mathcal{V}_L)$$

$$211 \quad \text{s.t. } \theta_{imp}^* = \arg \min_{\theta_{imp}} \mathcal{L}_{imp}(\theta_{imp}, \mathcal{V}_S)$$

214 where $\mathcal{L}_{bias}(\theta_{imp}^*, \mathcal{V}_S, \mathcal{V}_L)$ is computed based on labels instead of f_{class} . By minimizing the bias
 215 computed based on imputed values and labels, AMADB attempts to misguide any classifier that relies
 on such imputation to mitigate bias. AMADB is more tractable than AMFC, but still NP-hard.

216 **Theorem 1.** *The AMADB problem is NP-hard.*

218 See the proof in the Appendix. We frame AMADB as an adversarial version of *active learning* where
 219 the goal is to strategically minimize the accuracy of the imputation by selecting observed sensitive
 220 attributes. More specifically, we apply a popular formulation of active learning as a coverage problem
 221 (Yehuda et al., 2022; Ren et al., 2021). Theorem 1 can be interpreted as a positive result, as it shows
 222 that, in theory, a simpler surrogate of the adversary’s objective is still hard to optimize.

223 **A simple (yet effective) heuristic for adversarial missingness:** Let $s \in \{0, 1\}$ denote the true
 224 sensitive attribute and $\hat{s} \in \{0, 1\}$ be its imputation. We define the imputation error rate as $p(s \neq
 225 \hat{s}) = \epsilon$. Let $\hat{y} \in \{0, 1\}$ be the prediction of a fair model that minimizes demographic parity (ΔDP)
 226 with respect to \hat{s} , where we define ΔDP with respect to a sensitive attribute $a \in \{s, \hat{s}\}$ as follows:

$$227 \quad 228 \quad \Delta DP_a = |p(\hat{y} = 1|a = 0) - p(\hat{y} = 1|a = 1)|$$

229 We want to design a heuristic where the goal of the adversary is to choose missing values to maximize
 230 the difference between the true demographic parity ΔDP_s and empirical demographic parity $\Delta DP_{\hat{s}}$:

$$232 \quad \max_{\hat{s}} \Delta DP_s - \Delta DP_{\hat{s}} \\ 233 \quad = \max_{\hat{s}} |p(\hat{y} = 1|s = 0) - p(\hat{y} = 1|s = 1)| - |p(\hat{y} = 1|\hat{s} = 0) - p(\hat{y} = 1|\hat{s} = 1)|$$

235 We assume the minority class is underrepresented, i.e. $(\forall a, |p(\hat{y} = 1|a = 0) \geq p(\hat{y} = 1|a = 1)|)$:

$$237 \quad \max_{\hat{s}} p(\hat{y} = 1|s = 0) - p(\hat{y} = 1|s = 1) - p(\hat{y} = 1|\hat{s} = 0) + p(\hat{y} = 1|\hat{s} = 1) \\ 238 \quad = \max_{\hat{s}} p(\hat{y} = 1|s = 0) - p(\hat{y} = 1|\hat{s} = 0) + p(\hat{y} = 1|\hat{s} = 1) - p(\hat{y} = 1|s = 1) \\ 239 \quad = \max_{\hat{s}} p(\hat{y} = 1|s = 0) - p(\hat{y} = 1|\hat{s} = 0) + p(\hat{y} = 0|s = 1) - p(\hat{y} = 0|\hat{s} = 1)$$

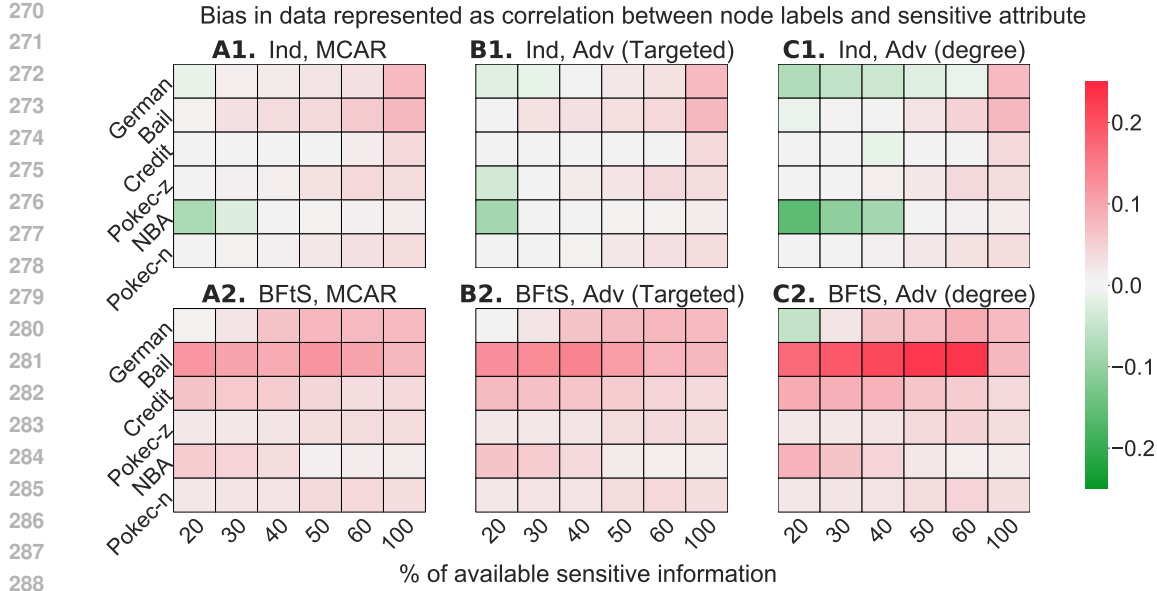
242 Assuming $p(\hat{y} \neq y) \rightarrow 0$, the adversary should attack nodes with $y = 1 \wedge s = 0$ and $y = 0 \wedge s = 1$
 243 to maximize $p(s \neq \hat{s}|y = 1, s = 0)$ and $p(s \neq \hat{s}|y = 0, s = 1)$. Based on Theorem 1, this problem is
 244 NP-hard. It also requires the adversary to have access to true class labels and sensitive values, which
 245 is a strong assumption. For practicality, we design an efficient adversary that aims to increase the
 246 imputation error $\epsilon = p(s \neq \hat{s})$ by exploiting the degree bias of GNNs using only the graph topology.

247 **Definition 3. The degree bias assumption:** Given nodes $u, v \in \mathcal{V}$ where $\deg(u) > \deg(v)$, we
 248 assume that $p(s_v \neq \hat{s}_v) > p(s_u \neq \hat{s}_u)$.

250 The degree bias assumption has been supported by both theoretical and empirical results in the
 251 literature for both homophilic and non-homophilic graphs (Tang et al., 2020; Liu et al., 2023; Ju et al.,
 252 2024; Subramonian et al., 2024). Moreover, low-degree nodes are known to be more vulnerable to
 253 attacks than high-degree nodes (Zügner et al., 2018; Zügner & Günnemann, 2019). Therefore, our
 254 adversarial missingness process simply selects low-degree nodes to have missing sensitive values.
 255 We call the heuristic based on the degree bias assumption the ‘degree’ heuristic.

256 We also consider another heuristic to evaluate the effectiveness of the degree one. We select missing
 257 values uniformly at random from the set $\mathcal{V}_{miss} = \{v \in \mathcal{V} | (y_v = 1 \wedge s_v = 0) \vee (y_v = 0 \wedge s_v = 1)\}$.
 258 If the desired number of missing nodes exceeds $|\mathcal{V}_{miss}|$, we draw the remaining $|\mathcal{V} \setminus \mathcal{V}_S| - |\mathcal{V}_{miss}|$
 259 samples uniformly at random from $\mathcal{V} \setminus \mathcal{V}_{miss}$. We call the resulting heuristic ‘targeted’.

260 To assess the effect of degree-based adversarial missingness, we compare imputation under adver-
 261 sarial degree, targeted and random missingness. Figure 2 reports correlations between sensitive
 262 attributes and class labels across datasets. Using a GCN for independent imputation, we observe
 263 that with less than 50% sensitive data, adversarial missingness consistently underestimates the true
 264 bias in the dataset, while random missingness and targeted missingness perform slightly better
 265 (Figures 2, top row). In contrast, BFTs (Figures 2, bottom row), introduced in the next section, rarely
 266 underestimates bias. These results highlight that off-the-shelf imputation can mislead fair graph
 267 learning by underestimating bias in the dataset, particularly under adversarial missingness. Among
 268 the three missingness processes, the degree heuristic exhibits the largest bias discrepancy between
 269 imputed and original values (i.e., is more adversarial). Therefore, we focus our analysis on the degree
 heuristic.



299 Figure 2: Empirical evaluation of three missingness processes and their effect on bias estimation.
 300 Degree-based adversarial missingness most effectively drives an independently trained GNN imputation
 301 model to underestimate bias, compared with random and targeted missingness. The final column in each matrix
 302 reports the true bias, where lower values indicate stronger underestimation. NBA shows the largest correlation
 303 gap (up to a 433% discrepancy when only 20% of protected attributes are observed) under the degree heuristic. We also include results for BFtS (Section 4), our 3-player
 304 adversarial imputation framework.

4 FAIRNESS-AWARE ADVERSARIAL MISSING DATA IMPUTATION

305 We introduce BFtS (Better Fair than Sorry), a 3-player adversarial framework for fair GNN training
 306 under adversarially missing sensitive data. The fair GNN is trained jointly with two adversaries—one
 307 to predict sensitive attributes based on GNN embeddings and another to impute missing values that
 308 minimize fairness, ensuring that fairness is evaluated against worst-case imputations.

309 We motivate the worst-case assumption using distributionally robust optimization (Ben-Tal et al.,
 310 2013; Mandal et al., 2020; Namkoong & Duchi, 2016; Shafieezadeh Abadeh et al., 2015). Let \mathcal{P}_s be
 311 the sensitive attribute distribution. We can express the fairness objective in terms of the expected bias.

$$\theta_{class}^* = \arg \min_{\theta_{class}} \mathcal{L}_{class} + \alpha \mathbb{E}_{s \sim \mathcal{P}_s} [\mathcal{L}_{bias}]$$

312 However, under adversarial missingness, the true distribution of sensitive values cannot be accurately
 313 estimated from the observations (Mohan et al., 2013; Tian, 2017). To handle this uncertainty, let us
 314 define an uncertainty set \mathcal{U} of plausible distributions for s . This leads to the worst-case imputation:

$$\theta_{class}^* = \arg \min_{\theta_{class}} \mathcal{L}_{class} + \alpha \max_{u \in \mathcal{U}} \mathbb{E}_{s \sim u} [\mathcal{L}_{bias}]$$

4.1 PROPOSED MODEL (BFtS)

315 Our goal is to learn a **group** fair and accurate GNN $\hat{y} = f_{class}(\mathcal{G}, \mathcal{X})$ for node classification with
 316 adversarially missing sensitive values. The proposed solution is model-agnostic (e.g., GNN) and
 317 based on adversarial learning. It formulates the imputation model as a second adversary of the GNN.
 318 Figure 3 depicts the flow diagram of the proposed model. The model has three primary components:
 319 a missing sensitive attribute imputation GNN f_{imp} , a node classification GNN f_{class} , and a sensitive
 320 attribute Deep Neural Net (DNN) prediction f_{bias} . f_{class} takes \mathcal{X} and \mathcal{G} as inputs and predicts the
 321 node labels. f_{bias} is an adversarial neural network that attempts to estimate the sensitive information
 322 from the final layer representations of f_{class} to assess the bias. More specifically, f_{class} is biased if
 323

324 the adversary f_{bias} can accurately predict the sensitive attribute information from the representations
 325 of f_{class} . The model f_{imp} predicts the missing sensitive attributes by taking \mathcal{X} and \mathcal{G} as inputs and
 326 generating the missing sensitive attributes \hat{s}_i . The goal of f_{imp} is to generate sensitive values that
 327 minimize the fairness of f_{class} , and, thus, it works as a second adversary to f_{class} .
 328

329 4.1.1 PLAYER ARCHITECTURES

330
 331 **GNN classifier** f_{class} : Node classi-
 332 fication model $\hat{y}_v = f_{class}(x_v, \mathcal{G})$ im-
 333 plemented using a GNN. We assume
 334 that f_{class} does not apply sensitive at-
 335 tributes but uses other attributes in \mathcal{X} that
 336 might be correlated with sensitive ones.
 337 The goal of f_{class} is to achieve
 338 both accuracy and fairness. To im-
 339 prove fairness, f_{class} tries to mini-
 340 mize the loss of adversary f_{bias} .
 341

342 **Sensitive attribute predictor (Adver-
 343 sary 1)** f_{bias} : Neural network that
 344 uses representations \mathbf{h}_v from f_{class} to
 345 predict sensitive attributes as $\hat{s}_a_v =$
 346 $f_{bias}(\mathbf{h}_v)$. f_{class} is fair if f_{bias} per-
 347 forms poorly.

348 **Missing data imputation GNN (Ad-
 349 versary 2)** f_{imp} : Predicts miss-
 350 ing sensitive attributes as $\hat{s}_i_v =$
 351 $f_{imp}(x_v, \mathcal{G})$. However, besides being
 352 accurate, f_{imp} plays the role of an ad-
 353 versary to f_{class} by predicting values
 354 that maximize the accuracy of f_{bias} .
 355

356 4.1.2 LOSS FUNCTIONS

357 **Node Classification:** We apply the
 358 cross-entropy loss to learn f_{class} as follows:

$$\mathcal{L}_{class} = -\frac{1}{|\mathcal{V}_L|} \sum_{v \in \mathcal{V}_L} \hat{y}_v \log(\hat{y}_v) + (1 - \hat{y}_v) \log(1 - \hat{y}_v). \quad (1)$$

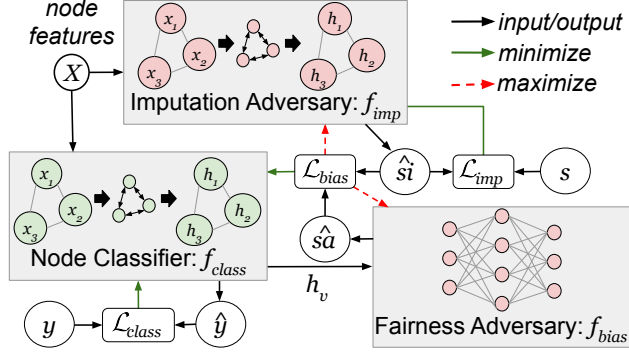
360 **Sensitive Attribute Imputation:** Because sensitive attributes tend to be imbalanced, f_{imp} applies
 361 the Label-Distribution-Aware Margin (LDAM) loss Cao et al. (2019). Let $\hat{s}_i = f_{imp}(X, \mathcal{G})$ be the
 362 one-hot encoded predictions and \hat{s}_i^s be the prediction for s_v . The LDAM loss of f_{imp} is defined as:
 363

$$\mathcal{L}_{imp} = \frac{1}{|\mathcal{V}_S|} \sum_{v=1}^{|\mathcal{V}_S|} -\log \frac{e^{\hat{s}_i^s - \Delta^s}}{e^{\hat{s}_i^s - \Delta^s} + \sum_{k \neq s} e^{\hat{s}_i^k}}. \quad (2)$$

364 where $\Delta^j = C/n_j^{\frac{1}{4}}$ and $j \in \{0, 1\}$, C is a constant independent of the sensitive attribute s , and n_j is
 365 the number of samples that belong to $s = j$.
 366

367 The LDAM loss is a weighted version of the negative log-likelihood loss. Intuitively, since Δ^j is
 368 larger for smaller values of n_j , and thus it ensures a higher margin for the smaller classes.
 369

370 **Sensitive attribute imputation with no sensitive information:** BFTS can generate fair outputs when
 371 very little or no sensitive information is provided by letting f_{imp} impute the sensitive values from
 372 the ground truth training labels y using the LDAM loss Du et al. (2021). More specifically, we
 373 replace \mathcal{V}_S with \mathcal{V}_L and s with y for each node $v \in \mathcal{V}_L$ in Eqn 2. The reasoning is that the worst-case
 374 fairness model generally assigns a more desired outcome to the non-sensitive group and a less desired
 375 outcome to the sensitive one. Therefore, the nodes predicted as the minority class will fall into the
 376 sensitive group, and vice versa. This is consistent with the worst-case assumption of BFTS.
 377



378 Figure 3: 3-player framework for fair GNN training with
 379 missing data imputation (BFTS). f_{class} generates node rep-
 380 resentations \mathbf{h}_v by minimizing the classification loss \mathcal{L}_{class}
 381 (Eqn. 1) and the maximizing sensitive attribute prediction
 382 loss \mathcal{L}_{bias} (Eqn. 3). f_{bias} predicts sensitive attributes using
 383 representations from f_{class} by minimizing \mathcal{L}_{bias} . f_{imp} pre-
 384 dicted missing values by minimizing the imputation loss \mathcal{L}_{imp}
 385 (Eqn. 2) and maximizing \mathcal{L}_{bias} . \hat{y} , \hat{s}_i , \hat{s}_a are predictions
 386 from f_{class} , f_{imp} and f_{bias} , respectively.

378 **Sensitive Attribute Prediction:** Given the sensitive information for \mathcal{V}_S , we first replace \hat{s}_v by s_v
 379 for $v \in \mathcal{V}_S$ and thereby generate \hat{s} . The parameters of f_{bias} are learned using:
 380

$$381 \quad \mathcal{L}_{bias} = \mathbb{E}_{\mathbf{h} \sim p(\mathbf{h}|\hat{s}=1)} [\log f_{bias}(\mathbf{h})] + \mathbb{E}_{\mathbf{h} \sim p(\mathbf{h}|\hat{s}=0)} [\log(1 - f_{bias}(\mathbf{h}))] \quad (3)$$

383 For simplicity, we consider a binary sensitive attribute in this paper. However, BFtS extends to
 384 non-binary or continuous sensitive attributes by appropriately generalizing the imputation loss \mathcal{L}_{imp}
 385 and the bias loss \mathcal{L}_{bias} to multi-class or continuous settings.
 386

387 4.1.3 LEARNING THE PARAMETERS OF BFtS

389 Let θ_{class} , θ_{bias} , and θ_{imp} be the parameters of f_{class} , f_{bias} , and f_{imp} , respectively, which are
 390 learned via a 3-player adversarial scheme described in Figure 3. Parameters θ_{class} are optimized as:
 391

$$392 \quad \theta_{class}^* = \arg \min_{\theta_{class}} \mathcal{L}_{class} + \alpha \mathcal{L}_{bias}. \quad (4)$$

393 where α is a hyperparameter that controls the trade-off between accuracy and fairness.
 394

395 The parameters of the sensitive attribute predictor θ_{bias} are learned by maximizing \mathcal{L}_{bias} :
 396

$$397 \quad \theta_{bias}^* = \arg \max_{\theta_{bias}} \mathcal{L}_{bias}. \quad (5)$$

398 To learn the parameters θ_{imp} of the imputation model to generate predictions that are accurate and
 399 represent the worst-case scenario for fairness, we apply the following:
 400

$$401 \quad \theta_{imp}^* = \arg \min_{\theta_{imp}} \mathcal{L}_{imp} - \beta \mathcal{L}_{bias}. \quad (6)$$

402 Here β is a hyperparameter that controls the trade-off between imputation accuracy and worst-case
 403 imputation. The min-max objective between the three players is therefore:
 404

$$405 \quad \min_{\theta_{class}} \max_{\theta_{imp}, \theta_{bias}} \mathbb{E}_{\mathbf{h} \sim p(\mathbf{h}|\hat{s}=1)} [\log f_{bias}(\mathbf{h})] + \mathbb{E}_{\mathbf{h} \sim p(\mathbf{h}|\hat{s}=0)} [\log(1 - f_{bias}(\mathbf{h}))]. \quad (7)$$

407 The training algorithm and time complexity analysis of BFtS are discussed in Appendix.
 408

409 4.2 THEORETICAL ANALYSIS

411 We will analyze some theoretical properties of BFtS. All the proofs are provided in Appendix.
 412

413 **Theorem 2.** *BFtS learns an imputation model f_{imp} with the worst-case imputation:*

$$415 \quad \theta_{imp}^* = \arg \max_{\theta_{imp}} \mathcal{L}_{bias} = \arg \max_{\theta_{imp}} |p(\hat{y} = 1|\hat{s} = 1) - p(\hat{y} = 1|\hat{s} = 0)|$$

417 where $\hat{y} = f_{class}(\mathcal{G}, \mathcal{X})$ and, $\hat{s} = f_{imp}(\mathcal{G}, \mathcal{X})$

418 The theorem shows that f_{imp} indeed generates imputations with minimum fairness (or maximum
 419 bias) based on Demographic Parity for a given classifier f_{class} .
 420

421 **Theorem 3.** *BFtS learns a classifier f_{class} that minimizes the worst-case bias:*

$$423 \quad \theta_{class}^* = \arg \min_{\theta_{class}} \sup_{\theta_{imp}} |p(\hat{y} = 1|\hat{s} = 1) - p(\hat{y} = 1|\hat{s} = 0)|$$

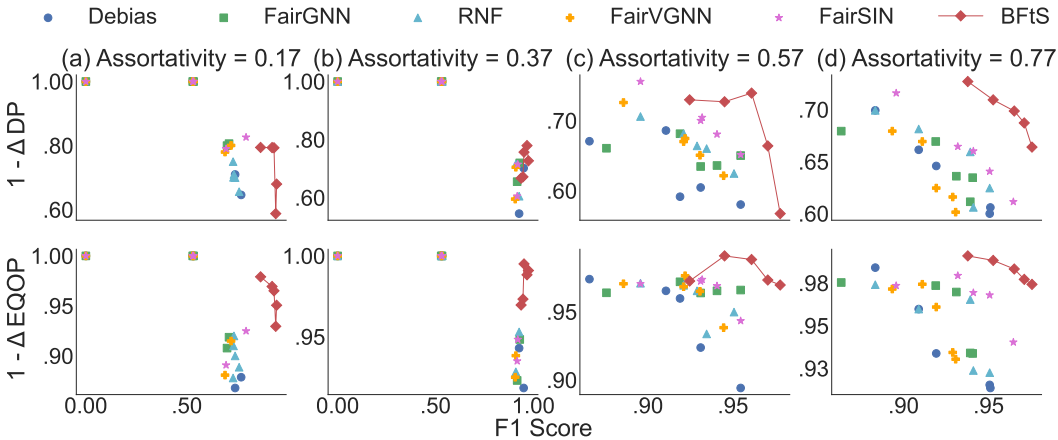
425 The optimal GNN classifier f_{class} , will achieve demographic parity ($\Delta DP = 0$ in Sec 5) for the
 426 worst-case imputation (minimum fairness) \hat{s} generated by f_{imp} . As f_{class} is a minimax estimator,
 427 the maximal ΔDP of BFtS is minimum amongst all estimators of s .
 428

429 **Corollary 1.** *Let $s' = f(G, X)$ be an imputation method independent of models f_{class} and f_{bias} ,
 then the BFtS imputation $\hat{s} = f_{imp}(\mathcal{G}, \mathcal{X})$ is such that:*

$$430 \quad JS(p(\mathbf{h}|s' = 1); p(\mathbf{h}|s' = 0)) \leq JS(p(\mathbf{h}|\hat{s} = 1); p(\mathbf{h}|\hat{s} = 0))$$

432 where JS is the *Jensen Shannon divergence*.
 433

434 The value of $JS(p(\mathbf{h}|s' = 1); p(\mathbf{h}|s' = 0))$ is related to the convergence of adversarial learning. For
 435 independent imputation, if s' is inaccurate, then $JS(p(\mathbf{h}|s' = 1); p(\mathbf{h}|s' = 0)) \approx 0$ and \mathcal{L}_{bias} in Eq.
 436 4 will be constant. The interplay between the three players makes BFtS more robust to convergence
 437 issues because the objective minimizes the upper bound on the JS divergence. This reduces the
 438 probability that the divergence vanishes during training (see details in the Appendix).



449 Figure 4: Performance of the methods using the SIMULATION dataset for different values of assortativity
 450 coefficients. In the x-axis, we plot the F1 score, and in the y-axis of the top row, we plot
 451 $1 - \Delta DP$, and in the y-axis of the bottom row, we plot $1 - \Delta EQOP$. The top right corner of the
 452 plot, therefore, represents a high F1 with low bias. When the assortativity is low, other methods fail
 453 to learn the node labels. With higher assortativity, though other methods learn the class labels, BFtS
 454 is less biased and has similar accuracy. Note that the X-axes have different ranges.

461 5 EXPERIMENTAL EVALUATION

462 We compare our approach (BFtS) against alternatives in terms of accuracy and fairness using real and
 463 synthetic data. We apply average precision (AVPR) and F1 for accuracy evaluation and ΔDP and
 464 $\Delta EQOP$ for fairness. Details about datasets, baselines, evaluation, and hyperparameters are provided
 465 in the Appendix. **We group the baselines into two categories.** First, we compare with methods that
 466 are explicitly designed to handle missing values: Debias Buyl & De Bie (2020), FairGNN Dai &
 467 Wang (2021), and RNF Du et al. (2021). Among these, RNF can operate when all sensitive attributes
 468 are missing, whereas Debias and FairGNN require access to at least some sensitive information.
 469 Both RNF and FairGNN rely on independent sensitive-attribute imputation procedures. Second, we
 470 compare our approach with state-of-the-art fair GNN models, including FairSIN Yang et al. (2024) and
 471 FairVGNN Wang et al. (2022). These methods cannot accommodate missing values directly, so we
 472 apply an independent imputation strategy consistent with the procedure used in FairGNN to supply the
 473 missing sensitive attributes before training. Additional experiments varying the GNN, scalability and
 474 complexity analysis using a synthetic large-scale graph, ablation studies (hyperparameter sensitivity,
 475 impact of LDAM loss, and impact of varying \mathcal{V}_S), and visualization of learnt representation and
 476 worst case assumption trade-off are also included in the Appendix. Our code can be found in an
 477 anonymous repository: <https://anonymous.4open.science/r/BFtS-6ADA>.

479 5.1 RESULTS AND ANALYSIS

480 Figure 4 shows the F1 score, $1 - \Delta DP$, and $1 - \Delta EQOP$ for different methods while varying
 481 their hyperparameters. The SIMULATION graph was generated using a stochastic block model with
 482 different assortativity coefficients, i.e., the extent to which links exist within clusters compared with
 483 across clusters. Learning missing sensitive values and node labels under low assortativity is hard, and
 484 graphs with assortativity 0.17 and 0.37 represent the scenario described in Corollary 1, therefore, the
 485 JS divergence tends to be small for independent imputation, which may result in a lack of convergence

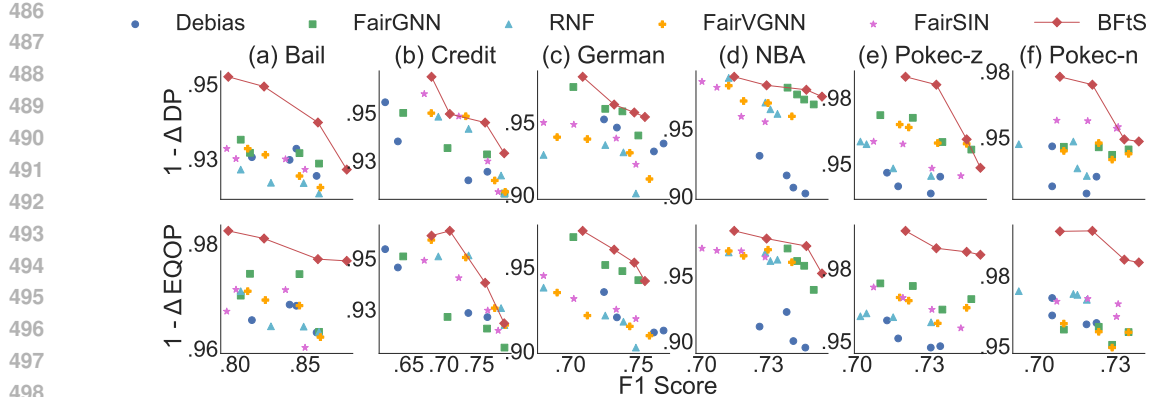


Figure 5: Fairness vs. accuracy results. The x-axis of each plot shows the F1 score. We plot $1 - \Delta DP$ and $1 - \Delta EQOP$ on the y-axis of rows 1 and 2, respectively. The top right corner of the plot represents a high F1 with low bias. BFtS often achieves better fairness for a similar value of F1.

	RNF				BFtS			
	%AVPR(\uparrow)	%F1(\uparrow)	% ΔDP (\downarrow)	% ΔEQ (\downarrow)	%AVPR(\uparrow)	%F1(\uparrow)	% ΔDP (\downarrow)	% ΔEQ (\downarrow)
BAIL	81.0 \pm 0.1	85.3 \pm 0.3	11.65 \pm 0.02	8.51 \pm 0.02	83.1 \pm 0.2	86.2 \pm 0.3	8.01 \pm 0.03	4.12 \pm 0.01
CREDIT	80.4 \pm 0.4	75.9 \pm 0.1	8.01 \pm 0.08	7.25 \pm 0.08	82.1 \pm 0.4	76.8 \pm 0.0	5.97 \pm 0.10	4.96 \pm 0.06
GERMAN	73.2 \pm 0.2	74.4 \pm 0.1	9.42 \pm 0.04	8.92 \pm 0.12	74.1 \pm 0.3	74.7 \pm 0.4	6.42 \pm 0.11	7.68 \pm 0.17
NBA	70.1 \pm 0.2	70.2\pm0.1	6.47 \pm 0.03	5.89 \pm 0.05	72.9 \pm 0.3	69.8 \pm 0.1	5.19\pm0.01	3.59 \pm 0.05
POKEC-Z	73.1 \pm 0.4	71.2 \pm 0.1	6.18 \pm 0.05	6.29 \pm 0.07	73.4 \pm 0.2	73.2 \pm 0.3	5.10\pm0.02	3.20 \pm 0.06
POKEC-N	71.6 \pm 0.2	72.2\pm0.1	7.58 \pm 0.01	7.09 \pm 0.04	72.6 \pm 0.1	69.6 \pm 0.4	4.29\pm0.02	3.01 \pm 0.03

Table 1: AVPR, F1, $\% \Delta DP$, and $\% \Delta EQOP$ without any sensitive information for BFtS and RNF (only baseline that operates in this setting). BFtS outperforms RNF in terms of fairness and accuracy.

for the baselines (FairGNN and Debias). As we increase the assortativity, all baselines can predict the labels, but BFtS still achieves a better fairness vs. accuracy trade-off in all cases.

We demonstrate the accuracy vs. fairness trade-off for real datasets in Figure 5. The top right corner of the plot represents high fairness and accuracy. Our model achieves better fairness and similar accuracy to the best baseline for the BAIL, NBA, GERMAN, POKEC-N and POKEC-Z. For all datasets, BFtS achieves a better fairness-accuracy tradeoff.

Table 1 shows the accuracy and fairness results for BAIL, CREDIT, GERMAN, POKEC-Z, POKEC-N and NBA without any sensitive attribute information. Among the baselines, only RNF works in this setting. BFtS outperforms RNF for the BAIL, GERMAN, and CREDIT. BFtS also outperforms RNF in terms of fairness on POKEC-Z, POKEC-N, and NBA with similar AVPR and F1.

BFtS outperforms the baselines because it effectively implements the worst-case assumption for missing value imputation. This assumption leads to stronger fairness guarantees (Theorem 3) than the baselines in cases where missing values are adversarial.

6 CONCLUSION

We investigate the challenge of incorporating fairness considerations into graph machine learning models when sensitive attributes are missing due to adversarial processes. Our solution is BFtS, a 3-player adversarial learning framework for the imputation of adversarially missing sensitive attributes that produce challenging values for graph-based fairness. Theoretical and empirical results demonstrate that BFtS achieves a better fairness \times accuracy trade-off than existing alternatives.

REPRODUCIBILITY STATEMENT

Details about datasets, baselines, evaluation, and hyperparameters are fully described in the Appendix. All real datasets and baselines applied in our experiments are publicly available. Our

540 code can be found in an anonymous repository: <https://anonymous.4open.science/r/BfTS-6ADA>.
 541
 542

543 REFERENCES
 544

545 Chirag Agarwal, Himabindu Lakkaraju, and Marinka Zitnik. Towards a unified framework for fair
 546 and stable graph representation learning. In *UAI*, 2021.
 547
 548 J Angwin, J Larson, S Mattu, and L Kirchner. Machine bias. Auerbach Publications, 2022.
 549
 550 Mario Arduini, Lorenzo Noci, Federico Pirovano, Ce Zhang, Yash Raj Shrestha, and Bibek Paudel.
 551 Adversarial learning for debiasing knowledge graph embeddings. *arXiv preprint*, 2020.
 552
 553 Aharon Ben-Tal, Dick Den Hertog, Anja De Waegenaere, Bertrand Melenberg, and Gijs Rennen.
 554 Robust solutions of optimization problems affected by uncertain probabilities. *Management
 555 Science*, 59(2):341–357, 2013.
 556
 557 Richard Berk, Hoda Heidari, Shahin Jabbari, Matthew Joseph, Michael Kearns, Jamie Morgen-
 558 stern, Seth Neel, and Aaron Roth. A convex framework for fair regression. *arXiv preprint
 559 arXiv:1706.02409*, 2017.
 560
 561 Derrick Blakely, Jack Lanchantin, and Yanjun Qi. Time and space complexity of graph convolutional
 562 networks. *Accessed on: Dec, 31:2021*, 2021.
 563
 564 Avishek Bose and William Hamilton. Compositional fairness constraints for graph embeddings. In
 565 *ICML*, 2019.
 566
 567 Samuel F Buck. A method of estimation of missing values in multivariate data suitable for use with
 568 an electronic computer. *Journal of the Royal Statistical Society: Series B*, 1960.
 569
 570 Maarten Buyl and Tijl De Bie. Debayes: a bayesian method for debiasing network embeddings. In
 571 *ICML*, 2020.
 572
 573 Kaidi Cao, Colin Wei, Adrien Gaidon, Nikos Arechiga, and Tengyu Ma. Learning imbalanced
 574 datasets with label-distribution-aware margin loss. In *NeurIPS*, 2019.
 575
 576 Junyi Chai and Xiaoqian Wang. Self-supervised fair representation learning without demographics.
 577 In *NeurIPS*, 2022.
 578
 579 Junyi Chai, Taeuk Jang, and Xiaoqian Wang. Fairness without demographics through knowledge
 580 distillation. In *NeurIPS*, 2022.
 581
 582 Robert S Chen, Brendan Lucier, Yaron Singer, and Vasilis Syrgkanis. Robust optimization for
 583 non-convex objectives. In *NeurIPS*, 2017.
 584
 585 Xu Chen, Siheng Chen, Jiangchao Yao, Huangjie Zheng, Ya Zhang, and Ivor W Tsang. Learning on
 586 attribute-missing graphs. *TPAMI*, 2020.
 587
 588 Eden Chlamtc, Michael Dinitz, and Yury Makarychev. Minimizing the union: Tight approximations
 589 for small set bipartite vertex expansion. In *Proceedings of the Twenty-Eighth Annual ACM-SIAM
 590 Symposium on Discrete Algorithms*, pp. 881–899. SIAM, 2017.
 591
 592 Enyan Dai and Suhang Wang. Say no to the discrimination: Learning fair graph neural networks
 593 with limited sensitive attribute information. In *WSDM*, 2021.
 594
 595 A. Rogier T. Donders, Geert J.M.G. van der Heijden, Theo Stijnen, and Karel G.M. Moons. A gentle
 596 introduction to imputation of missing values. *Journal of Clinical Epidemiology*, 2006.
 597
 598 Yushun Dong, Ninghao Liu, Brian Jalaian, and Jundong Li. Edits: Modeling and mitigating data bias
 599 for graph neural networks. In *WebConf*, 2022.
 600
 601 Yushun Dong, Jing Ma, Song Wang, Chen Chen, and Jundong Li. Fairness in graph mining: A survey.
 602 *TKDE*, (1):1–22, 2023.

594 Mengnan Du, Subhabrata Mukherjee, Guanchu Wang, Ruixiang Tang, Ahmed Awadallah, and Xia
 595 Hu. Fairness via representation neutralization. In *NeurIPS*, 2021.

596

597 Wei Fan, Kunpeng Liu, Rui Xie, Hao Liu, Hui Xiong, and Yanjie Fu. Fair graph auto-encoder for
 598 unbiased graph representations with wasserstein distance. In *ICDM*, 2021.

599 Michael Fauß, Abdelhak M Zoubir, and H Vincent Poor. Minimax robust detection: Classic results
 600 and recent advances. *IEEE TSP*, 2021.

601

602 Raymond Feng, Flavio P Calmon, and Hao Wang. Adapting fairness interventions to missing values.
 603 *arXiv preprint*, 2023.

604 Christian Fricke. Missing fairness: The discriminatory effect of missing values in datasets on fairness
 605 in machine learning. 2020.

606

607 Kazuto Fukuchi, Satoshi Hara, and Takanori Maehara. Faking fairness via stealthily biased sampling.
 608 In *Proceedings of the AAAI Conference on Artificial Intelligence*, volume 34, pp. 412–419, 2020.

609 Nicholas Furth, Abdallah Khreichah, Guanxiong Liu, NhatHai Phan, and Yasser Jararweh. Unfair
 610 trojan: Targeted backdoor attacks against model fairness. In *Handbook of Trustworthy Federated*
 611 *Learning*, pp. 149–168. Springer, 2024.

612

613 Malik Ghallab. Responsible ai: requirements and challenges. *AI Perspectives*, 2019.

614

615 AC Ghani, CA Donnelly, and GP Garnett. Sampling biases and missing data in explorations of sexual
 616 partner networks for the spread of sexually transmitted diseases. *Statistics in Medicine*, 1998.

617

618 Justin Gilmer, Samuel S Schoenholz, Patrick F Riley, Oriol Vinyals, and George E Dahl. Neural
 619 message passing for quantum chemistry. In *ICML*, 2017.

620

621 David Gray Grant. Equalized odds is a requirement of algorithmic fairness. *Synthese*, 201(3):101,
 622 2023.

623

624 Shubha Guha, Falaah Arif Khan, Julia Stoyanovich, and Sebastian Schelter. Automated data cleaning
 625 can hurt fairness in machine learning-based decision making. *IEEE Transactions on Knowledge
 626 and Data Engineering*, 36(12):7368–7379, 2024.

627

628 Dongliang Guo, Zhixuan Chu, and Sheng Li. Fair attribute completion on graph with missing
 629 attributes. *arXiv preprint arXiv:2302.12977*, 2023.

630

631 Moritz Hardt, Eric Price, and Nati Srebro. Equality of opportunity in supervised learning. In *NeurIPS*,
 632 2016.

633

634 Tatsunori Hashimoto, Megha Srivastava, Hongseok Namkoong, and Percy Liang. Fairness without
 635 demographics in repeated loss minimization. In *ICML*, 2018.

636

637 Hans Hofmann. Statlog (German Credit Data). UCI Machine Learning Repository, 1994.

638

639 Mark Huisman. Imputation of missing network data: Some simple procedures. *Journal of Social
 640 Structure*, 2009.

641

642 Hussain Hussain, Meng Cao, Sandipan Sikdar, Denis Helic, Elisabeth Lex, Markus Strohmaier, and
 643 Roman Kern. Adversarial inter-group link injection degrades the fairness of graph neural networks.
 644 In *2022 IEEE International Conference on Data Mining (ICDM)*, pp. 975–980. IEEE, 2022.

645

646 Haewon Jeong, Hao Wang, and Flavio P Calmon. Fairness without imputation: A decision tree
 647 approach for fair prediction with missing values. In *Proceedings of the AAAI Conference on
 648 Artificial Intelligence*, volume 36, pp. 9558–9566, 2022.

649

650 Kareem L Jordan and Tina L Freiburger. The effect of race/ethnicity on sentencing: Examining
 651 sentence type, jail length, and prison length. *Journal of Ethnicity in Criminal Justice*, 13(3):
 652 179–196, 2015.

653

654 Mingxuan Ju, Tong Zhao, Wenhao Yu, Neil Shah, and Yanfang Ye. Graphpatcher: mitigating degree
 655 bias for graph neural networks via test-time augmentation. In *NeurIPS*, 2024.

648 Faisal Kamiran and Toon Calders. Classifying without discriminating. In *ICCC*, 2009.
 649

650 Jian Kang, Yinglong Xia, Ross Maciejewski, Jiebo Luo, and Hanghang Tong. Deceptive fairness
 651 attacks on graphs via meta learning. *arXiv preprint arXiv:2310.15653*, 2023.

652 Ahmad Khajehnejad, Moein Khajehnejad, Mahmoudreza Babaei, Krishna Gummadi, Adrian Weller,
 653 and Baharan Mirzasoleiman. Crosswalk: Fairness-enhanced node representation learning. In *AAAI*,
 654 2022.

655 Deniz Koyuncu, Alex Gittens, Bülent Yener, and Moti Yung. Deception by omission: Using
 656 adversarial missingness to poison causal structure learning. In *Proceedings of the 29th ACM*
 657 *SIGKDD Conference on Knowledge Discovery and Data Mining*, pp. 1164–1175, 2023.

658 Deniz Koyuncu, Alex Gittens, Bülent Yener, and Moti Yung. Adversarial missingness attacks on
 659 causal structure learning. *ACM Transactions on Intelligent Systems and Technology*, 15(6):1–60,
 660 2024.

661 C Laclau, I Redko, M Choudhary, and C Largeron. All of the fairness for edge prediction with
 662 optimal transport. In *AISTATS*, 2021.

663

664 Preethi Lahoti, Alex Beutel, Jilin Chen, Kang Lee, Flavien Prost, Nithum Thain, Xuezhi Wang, and
 665 Ed Chi. Fairness without demographics through adversarially reweighted learning. In *NeurIPS*,
 666 2020.

667 Gert RG Lanckriet, Laurent El Ghaoui, Chiranjib Bhattacharyya, and Michael I Jordan. A robust
 668 minimax approach to classification. *JMLR*, 2002.

669

670 Hongyi Ling, Zhimeng Jiang, Youzhi Luo, Shuiwang Ji, and Na Zou. Learning fair graph representa-
 671 tions via automated data augmentations. In *ICLR*, 2023.

672

673 Roderick JA Little and Donald B Rubin. *Statistical analysis with missing data*. John Wiley & Sons,
 674 2019.

675

676 Zemin Liu, Trung-Kien Nguyen, and Yuan Fang. On generalized degree fairness in graph neural
 677 networks. In *AAAI*, 2023.

678

679 Johan Löfberg. *Minimax approaches to robust model predictive control*. Linköping University, 2003.

680

681 Elizabeth Luh. Not so black and white: Uncovering racial bias from systematically misreported
 682 trooper reports. *Available at SSRN 3357063*, 2022.

683

684 Zihan Luo, Hong Huang, Yongkang Zhou, Jiping Zhang, Nuo Chen, and Hai Jin. Are your models
 685 still fair? fairness attacks on graph neural networks via node injections. In *The Thirty-eighth*
 686 *Annual Conference on Neural Information Processing Systems*, 2024.

687

688 David Madras, Elliot Creager, Toniann Pitassi, and Richard Zemel. Learning adversarially fair and
 689 transferable representations. In *International Conference on Machine Learning*, pp. 3384–3393.
 690 PMLR, 2018.

691

692 Debmalya Mandal, Samuel Deng, Suman Jana, Jeannette Wing, and Daniel J Hsu. Ensuring fairness
 693 beyond the training data. 2020.

694

695 Haris Mansoor, Sarwan Ali, Shafiq Alam, Muhammad Asad Khan, Umair Ul Hassan, and Imdadullah
 696 Khan. Impact of missing data imputation on the fairness and accuracy of graph node classifiers. In
 697 *BigData*, 2022.

698

699 Fernando Martínez-Plumed, Cèsar Ferri, David Nieves, and José Hernández-Orallo. Fairness and
 700 missing values. *arXiv preprint arXiv:1905.12728*, 2019.

701

Ninareh Mehrabi, Muhammad Naveed, Fred Morstatter, and Aram Galstyan. Exacerbating algorithmic
 702 bias through fairness attacks. In *Proceedings of the AAAI Conference on Artificial Intelligence*,
 703 volume 35, pp. 8930–8938, 2021.

702 Arpit Merchant and Carlos Castillo. Disparity, inequality, and accuracy tradeoffs in graph neural
 703 networks for node classification. In *CIKM*, 2023.

704

705 Karthika Mohan, Judea Pearl, and Jin Tian. Graphical models for inference with missing data.
 706 *Advances in neural information processing systems*, 26, 2013.

707

708 Hongseok Namkoong and John C Duchi. Stochastic gradient methods for distributionally robust
 709 optimization with f-divergences. *Advances in neural information processing systems*, 29, 2016.

710

711 Tu Nguyen, Trung Le, Hung Vu, and Dinh Phung. Dual discriminator generative adversarial nets.
 712 *NeurIPS*, 2017.

713

714 William P O'Hare and William P O'Hare. Potential explanations for why people are missed in the us
 715 census. *Differential Undercounts in the US Census: Who is Missed?*, 2019.

716

717 John Palowitch and Bryan Perozzi. Monet: Debiasing graph embeddings via the metadata-orthogonal
 718 training unit. *arXiv preprint*, 2019.

719

720 Ricardo Cardoso Pereira, Miriam Seoane Santos, Pedro Pereira Rodrigues, and Pedro Henriques
 721 Abreu. Reviewing autoencoders for missing data imputation: Technical trends, applications and
 722 outcomes. *JAIR*, 2020.

723

724 Dana Pessach and Erez Shmueli. A review on fairness in machine learning. *CSUR*, 2022.

725

726 Tahleen Rahman, Bartłomiej Surma, Michael Backes, and Yang Zhang. Fairwalk: towards fair graph
 727 embedding. In *AAAI*, 2019.

728

729 Pengzhen Ren, Yun Xiao, Xiaojun Chang, Po-Yao Huang, Zhihui Li, Brij B Gupta, Xiaojiang Chen,
 730 and Xin Wang. A survey of deep active learning. *ACM computing surveys (CSUR)*, 54(9):1–40,
 731 2021.

732

733 Emanuele Rossi, Henry Kenlay, Maria I Gorinova, Benjamin Paul Chamberlain, Xiaowen Dong, and
 734 Michael Bronstein. On the unreasonable effectiveness of feature propagation in learning on graphs
 735 with missing node features. *arXiv preprint*, 2021.

736

737 Soroosh Shafieezadeh Abadeh, Peyman M Mohajerin Esfahani, and Daniel Kuhn. Distributionally
 738 robust logistic regression. *Advances in neural information processing systems*, 28, 2015.

739

740 Shai Shalev-Shwartz and Yonatan Wexler. Minimizing the maximal loss: How and why. In *ICML*,
 741 2016.

742

743 David Solans, Battista Biggio, and Carlos Castillo. Poisoning attacks on algorithmic fairness. In
 744 *Joint European Conference on Machine Learning and Knowledge Discovery in Databases*, pp.
 745 162–177. Springer, 2020.

746

747 I Spinelli, S Scardapane, A Hussain, and A Uncini. Fairdrop: Biased edge dropout for enhancing
 748 fairness in graph representation learning. *TAI*, 2021.

749

750 Arjun Subramonian, Kai-Wei Chang, and Yizhou Sun. On the discrimination risk of mean aggregation
 751 feature imputation in graphs. In *NeurIPS*, 2022.

752

753 Arjun Subramonian, Jian Kang, and Yizhou Sun. Theoretical and empirical insights into the origins
 754 of degree bias in graph neural networks. *Advances in Neural Information Processing Systems*, 37:
 755 8193–8239, 2024.

756

757 Lubos Takac and Michal Zabovsky. Data analysis in public social networks. In *DTI*, 2012.

758

759 Xianfeng Tang, Huaxiu Yao, Yiwei Sun, Yiqi Wang, Jiliang Tang, Charu Aggarwal, Prasenjit Mitra,
 760 and Suhang Wang. Investigating and mitigating degree-related biases in graph convolutional
 761 networks. In *CIKM*, 2020.

762

763 Hoang Thanh-Tung and Truyen Tran. Catastrophic forgetting and mode collapse in gans. In *2020
 764 international joint conference on neural networks (ijcnn)*, pp. 1–10. IEEE, 2020.

756 Jin Tian. Recovering probability distributions from missing data. In *Asian Conference on Machine*
 757 *Learning*, pp. 574–589. PMLR, 2017.

758

759 Simon Vandenhende, Bert De Brabandere, Davy Neven, and Luc Van Gool. A three-player gan:
 760 generating hard samples to improve classification networks. In *MVA*, 2019.

761

762 Petar Velickovic, Guillem Cucurull, Arantxa Casanova, Adriana Romero, Pietro Lio, Yoshua Bengio,
 763 et al. Graph attention networks. *stat*, 1050(20):10–48550, 2017.

764

765 Neil Vigdor. Apple card investigated after gender discrimination complaints. *New York Times*, 2019.

766

767 Wang et al. Improving fairness in graph neural networks via mitigating sensitive attribute leakage. In
 768 *KDD*, 2022.

769

770 Ann M Weber, Ribhav Gupta, Safa Abdalla, Beniamino Cislagli, Valerie Meausoone, and Gary L
 771 Darmstadt. Gender-related data missingness, imbalance and bias in global health surveys. *BMJ*
 772 *Global Health*, 2021.

773

774 Lilian Weng. From gan to wgan. *arXiv preprint arXiv:1904.08994*, 2019.

775

776 Shen Yan, Hsien-te Kao, and Emilio Ferrara. Fair class balancing: Enhancing model fairness without
 777 observing sensitive attributes. In *CIKM*, 2020.

778

779 Cheng Yang, Jixi Liu, Yunhe Yan, and Chuan Shi. Fairsin: Achieving fairness in graph neural
 780 networks through sensitive information neutralization. In *AAAI*, 2024.

781

782 I-Cheng Yeh and Che-hui Lien. The comparisons of data mining techniques for the predictive
 783 accuracy of probability of default of credit card clients. *Expert systems with applications*, 36(2):
 784 2473–2480, 2009.

785

786 Ofer Yehuda, Avihu Dekel, Guy Hacohen, and Daphna Weinshall. Active learning through a covering
 787 lens. *Advances in Neural Information Processing Systems*, 35:22354–22367, 2022.

788

789 Binchi Zhang, Yushun Dong, Chen Chen, Yada Zhu, Minnan Luo, and Jundong Li. Adversarial
 790 attacks on fairness of graph neural networks. *arXiv preprint arXiv:2310.13822*, 2023.

791

792 Brian Hu Zhang, Blake Lemoine, and Margaret Mitchell. Mitigating unwanted biases with adversarial
 793 learning. In *AIES*, 2018.

794

795 Yiliang Zhang and Qi Long. Assessing fairness in the presence of missing data. In *NeurIPS*, 2021.

796

797 Yiliang Zhang and Qi Long. Fairness-aware missing data imputation. In *Workshop on Trustworthy
 798 and Socially Responsible Machine Learning, NeurIPS 2022*, 2022.

799

800 Zhilu Zhang and Mert Sabuncu. Generalized cross entropy loss for training deep neural networks
 801 with noisy labels. In *NeurIPS*, 2018.

802

803 Tianxiang Zhao, Enyan Dai, Kai Shu, and Suhang Wang. Towards fair classifiers without sensitive
 804 attributes: Exploring biases in related features. In *WSDM*, 2022.

805

806 Mengxin Zheng, Jiaqi Xue, Yi Sheng, Lei Yang, Qian Lou, and Lei Jiang. Trojfair: trojan fairness
 807 attacks. *arXiv preprint arXiv:2312.10508*, 2023.

808

809 Yuchang Zhu, Jintang Li, Zibin Zheng, and Liang Chen. Fair graph representation learning via
 810 sensitive attribute disentanglement. In *Proceedings of the ACM Web Conference 2024*, pp. 1182–
 811 1192, 2024.

812

813 Daniel Zügner and Stephan Günnemann. Certifiable robustness and robust training for graph
 814 convolutional networks. In *Proceedings of the 25th ACM SIGKDD international conference on
 815 knowledge discovery & data mining*, pp. 246–256, 2019.

816

817 Daniel Zügner, Amir Akbarnejad, and Stephan Günnemann. Adversarial attacks on neural networks
 818 for graph data. In *Proceedings of the 24th ACM SIGKDD international conference on knowledge
 819 discovery & data mining*, pp. 2847–2856, 2018.

810 A TECHNICAL APPENDICES AND SUPPLEMENTARY MATERIAL
811812 This supplementary material includes the following:
813

- 814 • Details of Graph Neural Network (GNN)
- 815 • Evaluation Metrics
- 816 • Dataset Details
- 817 • Baselines
- 818 • Software and Hardware
- 819 • Hyperparameter Setting
- 820 • Proof of theorems and corollaries
- 821 • Training algorithm
- 822 • Complexity and Running time comparison
- 823 • Imputation accuracy
- 824 • Worst case fairness accuracy trade-off
- 825 • Additional experiments
- 826 • Ablation Study

830 GRAPH NEURAL NETWORK
831832 Two of the models (or players) learned by our model are GNNs. Without loss of generality, we will
833 assume that they are message-passing neural networks (Gilmer et al., 2017), which we will simply
834 refer to as GNNs. A GNN learns node representations \mathbf{h}_v for each node v that can be used to predict
835 (categorical or continuous) values $y_v = f(\mathbf{h}_v)$. These representations are learned via successive
836 AGGREGATE and COMBINE operations defined as follows:

837
$$\mathbf{h}_v^k = \text{COMBINE}^k(\mathbf{h}_v^{k-1}, \text{AGGREGATE}^{k-1}(\mathbf{h}_u^{k-1}, A_{u,v} = 1)).$$

838 where \mathbf{a}_v^k aggregates the messages received by the neighbors of v in \mathcal{G} and \mathbf{h}_v^k are representations
839 learned at the k -th layer.
840841 EVALUATION METRICS
842843 **Utility Evaluation:** As with many datasets in the fairness literature, our datasets are imbalanced. To
844 evaluate their accuracy, we apply average precision (AVPR) and the F1 score.
845846 **Fairness Evaluation:** We apply two bias metrics that will be defined based on a sensitive attribute
847 s . Let $s = 1$ be the sensitive group and $s = 0$ be the non-sensitive group. The *Demographic Parity*
848 (*DP*) requires the prediction to be independent of the sensitive attribute (Kamiran & Calders, 2009).
849 We evaluate demographic parity as:

850
$$\Delta DP(\hat{y}, s) = |p(\hat{y} = 1|s = 1) - p(\hat{y} = 1|s = 0)|. \quad (8)$$

851 *Equality of Opportunity (EQOP)* calculates the difference between true positive rates between
852 sensitive and non-sensitive groups (Hardt et al., 2016) as follows:
853

854
$$\Delta EQOP(\hat{y}, s, y) = |p(\hat{y} = 1|s = 1, y = 1) - p(\hat{y} = 1|s = 0, y = 1)|. \quad (9)$$

855 *Equalized Odds (EQODDS)* calculates the average difference between true positive rates and false
856 positive rates between sensitive and non-sensitive groups (Grant, 2023) as follows:
857

$$\Delta EQODDS(\hat{y}, s, y) = \frac{1}{2} |p(\hat{y} = 1|s = 1, y = 1) - p(\hat{y} = 1|s = 0, y = 1)| + \\ 858 \quad |p(\hat{y} = 1|s = 1, y = 0) - p(\hat{y} = 1|s = 0, y = 0)|. \quad (10)$$

859 We can get corresponding fairness by subtracting ΔDP and $\Delta EQOP$ from 1.
860861 We use ΔDP and $\Delta EQOP$ for most of our analysis as they are commonly used group-based metrics
862 in fairness literature. Our theoretical analysis guarantees Demographic Parity, but we can change the
863 \mathcal{L}_{bias} loss to account for a different type of fairness Madras et al. (2018).

864
865

DATASET DETAILS

866
867
868
869
870
871
872
873
874

SIMULATION: We simulate a synthetic graph consisting of 1000 nodes based on the stochastic block model with blocks of sizes 600 and 400, for the majority and minority classes, respectively. We can have different edge probabilities within and across blocks and generate graphs with different assortativity coefficients. The sensitive attribute s is simulated as $s \sim Bernoulli(p)$ if $y = 1$ and $s \sim Bernoulli(1 - p)$ otherwise. The probability $p = 0.5$ generates a random assignment of the sensitive attribute, while p close to 1 or 0 indicates an extremely biased scenario. For our simulation, we use $p = 0.7$ so that the dataset is unfair. Each node has 20 attributes, of which 8 are considered noisy. The noisy attributes are simulated as $Normal(0, 1)$ and the remaining ones as $\gamma * y + Normal(0, 1)$, where γ is the strength of the signal in important features.

875
876
877
878
879
880

BAIL (Jordan & Freiburger, 2015): Contains 18,876 nodes representing people who committed a criminal offense and were granted bail by US state courts between 1990 and 2009. Defendants are linked based on similarities in their demographics and criminal histories. The objective is to categorize defendants as likely to post bail vs. no bail. No-bail defendants are expected to be more likely to commit violent crimes if released. Race information is considered a sensitive attribute. Features include education, marital status, and profession.

881
882
883
884

CREDIT (Yeh & Lien, 2009): The dataset has 30,000 nodes representing people each with 25 features, including education, total overdue counts, and most recent payment amount. The objective is to forecast if a person will or won't miss a credit card payment while considering age as a sensitive attribute. Nodes are connected based on payment patterns and spending similarities.

885
886
887

GERMAN (Hofmann, 1994): The dataset consists of 1000 nodes and 20 features (e.g., credit amount, savings) representing clients at a German bank. Labels are credit decisions for a person (good or bad credit). The sensitive attribute is gender. The goal is to predict who should receive credit.

888
889
890
891

NBA (Dai & Wang, 2021): Dataset based on a Kaggle dataset about the National Basketball Association (US). It contains 403 players as nodes connected based on their Twitter activity. Attributes represent player statistics and nationality is considered the sensitive attribute. The goal is to predict the players' salaries (above/under the median).

892
893
894
895

POKEC (Takac & Zabovsky, 2012): This dataset has two variations: POKEC-Z and POKEC-N. The pokec dataset is based on a popular social network in Slovakia. The sensitive attribute in POKEC-Z and POKEC-N are two different regions of Slovakia. The goal is to predict the working field of users.

896
897

BASELINES

898
899
900

Vanilla: The vanilla model is the basic GNN model trained with cross-entropy loss without any fairness intervention.

901
902
903
904

Debias (Zhang et al., 2018): Debias is an adversarial learning method that trains a classifier and an adversary simultaneously. The adversary is trained using the softmax output of the last layer of the classifier. It does not handle missing sensitive data. Hence, we only use $\mathcal{V}_S \in \mathcal{V}$ to calculate the adversarial loss.

905
906
907

FairGNN (Dai & Wang, 2021): FairGNN first uses a GNN to estimate the missing sensitive attributes. It then trains another GNN-based classifier and a DNN adversary. The adversary helps to eliminate bias from the representations learned by the GNN classifier.

908
909
910
911

RNF (Du et al., 2021): RNF imputes the missing sensitive attributes by first training the model with generalized cross entropy (Zhang & Sabuncu, 2018). It eliminates bias from the classification head. RNF uses samples with the same ground-truth label but distinct sensitive attributes and trains the classification head using their neutralized representations.

912
913
914
915

FairVGNN (Wang et al., 2022): FairVGNN learns fair node representations via automatically identifying and masking sensitive-correlated features. It requires complete sensitive information, so we use the same imputation method as FairGNN for the missing values.

916
917

FairSIN (Yang et al., 2024): FairSIN learns fair representations by adding additional fairness-facilitating features. It also requires complete sensitive information, so we use the same independent imputation method as FairGNN for the missing values. (Yang et al., 2024):

918 SOFTWARE AND HARDWARE
919
920 • Operating System: Linux (Red Hat Enterprise Linux 8.9 (Ootpa))
921 • GPU: NVIDIA A40
922 • Software: Python 3.8.10, torch 2.2.1, dgl==0.4.3
923
924 HYPERPARAMETER SETTINGS
925
926 The size of \mathcal{V}_S was set to 30% of $|\mathcal{V}|$ unless stated otherwise. Each GNN has two layers and a
927 dropout probability of 0.5. In practice, some sensitive information is often available, unless otherwise
928 stated. Therefore, we concentrate the majority of our experiments on the assumption that there
929 is a limited amount of sensitive information available, and we generate the imputations using the
930 available sensitive information in Equation 2. The \mathcal{V}_S was set to 30% for all experiments unless stated
931 otherwise. \mathcal{V}_L is 300, 400, 1400, 100, 500, 500, and 800 for the SIMULATION, GERMAN, CREDIT,
932 NBA, POKEC-Z, POKEC-N and BAIL datasets, respectively. We adjust the values of α and β for
933 each dataset using cross-validation based on the F1 score. For all baselines, we choose the respective
934 regularizers using cross-validation based on the same metrics. Every model, except RNF, combines
935 the training of several networks with various convergence rates. We stop training RNF based on early
936 stopping to eliminate overfitting. We train the rest of the models for certain epochs and choose the
937 model with the best AVPR. All the results shown in the following section are the average of 10 runs.
938 We use GCN as the GNN architecture for all experiments unless mentioned otherwise.
939
940 PROOF OF THEOREMS
941942 THEOREM 1
943
944 We will consider an adversarial active learning setting, where the goal of the adversary is to select k
945 labels (i.e., observed sensitive values) to minimize the bias \mathcal{L}_{bias} of the data imputed by f_{imp} . More
946 specifically, our proof will use the coverage model for active learning, where an unlabeled data point
947 x_i^u can be correctly predicted iff it is covered by at least one labeled point x_j^l . The goal is for the
948 labeled points $\{x_1^l, x_2^l, \dots, x_k^l\}$ to cover as many unlabeled data points $\{x_1^u, x_2^u, \dots, x_{n-k}^u\}$ as possible
949 (Yehuda et al., 2022; Ren et al., 2021). Thus, in our setting, the adversary’s goal is to select labels to
950 minimize the coverage of the following sets of nodes: (1) nodes in the sensitive group ($s_v = 1$) and
951 the negative class ($y = 0$) and (2) nodes in the non-sensitive group ($s_v = 0$) and the positive class
952 ($y = 1$). This can be achieved by minimizing the coverage of such nodes. We provide a reduction
953 from the *minimum k-union problem*.
954

955 **Minimum k-union problem (MkU, Chlamtc et al. (2017)):** Given a set of sets $\mathcal{S} = S_1, S_2, \dots, S_q$,
956 where each set $S_i \subseteq \mathcal{I}$ and \mathcal{I} is a set of items. The problem consists of selecting r sets S_1, S_2, \dots, S_r
957 from \mathcal{S} to minimize the coverage $S_1 \cap S_2 \cap \dots \cap S_r$.
958

959 Under our coverage model, the reduction is straightforward. Given an instance of *MkU*, we define
960 a corresponding instance of the *Adversarial Missingness against Data Bias* (AMADB) problem as
961 follows. We represent each item in \mathcal{I} and each set in \mathcal{S} as a data point x and assign all data points to
962 both the non-sensitive group ($s_v = 0$) and the positive class ($y = 1$). Moreover, we will add one data
963 point x' that will belong to the sensitive group ($s_v = 1$) and the positive class ($y = 1$). Therefore, the
964 resulting set of data points is $\{x_1, x_2, \dots, x_n\}$, where $n = |\mathcal{S}| + |\mathcal{I}| + 1$. Moreover, let x_i cover x_j
965 iff x_i represents a set $S_i \in \mathcal{S}$, x_j represents an item $i_j \in \mathcal{I}$, and $i_j \in S_i$. It follows that minimizing
966 the bias in the AMADB instance by selecting data points x_j to be labeled is equivalent to minimizing
967 the coverage in the corresponding *MkU* instance.
968
969 THEOREM 2
970
971 *Proof.* From Eq. 7, the min-max objective of BFtS is:
972

$$\begin{aligned} & \mathbb{E}_{\mathbf{h} \sim p(\mathbf{h}|\hat{s}=1)} [\log(f_{bias}(\mathbf{h}))] + \mathbb{E}_{\mathbf{h} \sim p(\mathbf{h}|\hat{s}=0)} [\log(1 - f_{bias}(\mathbf{h}))] \\ &= \sum_h p(\mathbf{h}|\hat{s}=1) \log(f_{bias}(\mathbf{h})) + \sum_h p(\mathbf{h}|\hat{s}=0) \log(1 - f_{bias}(\mathbf{h})) \end{aligned}$$

972 If we fix θ_{class} and θ_{imp} , then the optimal f_{bias} is $\frac{p(\mathbf{h}|\hat{s}=1)}{p(\mathbf{h}|\hat{s}=1)+p(\mathbf{h}|\hat{s}=0)}$. By substituting the optimal
 973 f_{bias} in Eq. 7 we get:
 974

$$\begin{aligned} 975 \min_{\theta_{class}} \max_{\theta_{imp}} \mathbb{E}_{\mathbf{h} \sim p(\mathbf{h}|\hat{s}=1)} [\log \frac{p(\mathbf{h}|\hat{s}=1)}{p(\mathbf{h}|\hat{s}=1)+p(\mathbf{h}|\hat{s}=0)}] + \\ 976 \\ 977 \mathbb{E}_{\mathbf{h} \sim p(\mathbf{h}|\hat{s}=0)} [\log (1 - \frac{p(\mathbf{h}|\hat{s}=1)}{p(\mathbf{h}|\hat{s}=1)+p(\mathbf{h}|\hat{s}=0)})] \\ 978 \end{aligned}$$

979 We further simplify the objective function and get:
 980

$$\begin{aligned} 981 \mathbb{E}_{\mathbf{h} \sim p(\mathbf{h}|\hat{s}=1)} [\log \frac{p(\mathbf{h}|\hat{s}=1)}{p(\mathbf{h}|\hat{s}=1)+p(\mathbf{h}|\hat{s}=0)}] + \\ 982 \\ 983 \mathbb{E}_{\mathbf{h} \sim p(\mathbf{h}|\hat{s}=0)} [\log \frac{p(\mathbf{h}|\hat{s}=0)}{p(\mathbf{h}|\hat{s}=1)+p(\mathbf{h}|\hat{s}=0)}] \\ 984 \\ 985 = \sum_h p(\mathbf{h}|\hat{s}=1) \log \frac{p(\mathbf{h}|\hat{s}=1)}{p(\mathbf{h}|\hat{s}=1)+p(\mathbf{h}|\hat{s}=0)} + \\ 986 \\ 987 \sum_h p(\mathbf{h}|\hat{s}=0) \log \frac{p(\mathbf{h}|\hat{s}=0)}{p(\mathbf{h}|\hat{s}=1)+p(\mathbf{h}|\hat{s}=0)} \\ 988 \\ 989 = -\log 4 + 2JS(p(\mathbf{h}|\hat{s}=1); p(\mathbf{h}|\hat{s}=0)) \\ 990 \\ 991 \end{aligned}$$

992 By removing the constants, we can further simplify the min-max optimization with optimal f_{bias} to:
 993

$$\min_{\theta_{class}} \max_{\theta_{imp}} JS(p(\mathbf{h}|\hat{s}=1); p(\mathbf{h}|\hat{s}=0))$$

994 The optimal f_{imp} thereby maximizes the following objective:
 995

$$JS(p(\mathbf{h}|\hat{s}=1); p(\mathbf{h}|\hat{s}=0))$$

996 Since $\hat{y} = \sigma(\mathbf{h} \cdot \mathbf{w})$, f_{imp} generates imputation so that
 997

$$\min_{\theta_{class}} \sup_{\hat{s}} JS(p(\hat{y}|\hat{s}=1); p(\hat{y}|\hat{s}=0))$$

998 The supremum value will make the two probabilities maximally different. Therefore, for the optimal
 999 f_{imp} we get,
 1000

$$\min_{\theta_{class}} \sup_{\hat{s}} |p(\hat{y}|\hat{s}=1) - p(\hat{y}|\hat{s}=0)|$$

1001 Let $\Delta DP_{\theta_{class}, \theta_{imp}} = |p(\hat{y}=1|\hat{s}=1) - p(\hat{y}=1|\hat{s}=0)|$, then, the optimal θ_{imp}^* generates the
 1002 worst-case (minimum fairness) imputation so that $\Delta DP_{\theta_{class}, \theta_{imp}^*} \geq \Delta DP_{\theta_{class}, \theta_{imp}}$ \square
 1003

1004 THEOREM 3

1005 *Proof.* From Theorem 1, we get,
 1006

$$\min_{\theta_{class}} \sup_{\hat{s}} |p(\hat{y}|\hat{s}=1) - p(\hat{y}|\hat{s}=0)|$$

1007 Let us assume that there can be m different \hat{s} that produce sensitive attributes $\hat{s}_1, \hat{s}_2, \dots, \hat{s}_m$. If we let
 1008 D_i be the uniform distribution over each s_i , then BFtS minimizes the $|p(\hat{y}|\hat{s}=1) - p(\hat{y}|\hat{s}=0)|$ in
 1009 the worst case over these different distributions D_i . Therefore, f_{class} is a minimax estimator. The
 1010 objective of Eq. 7 with optimal $\theta_{bias}^*, \theta_{imp}^*$ and f_{class}^* becomes:
 1011

$$\inf_{\hat{y}} \sup_{\hat{s}} |p(\hat{y}|\hat{s}=1) - p(\hat{y}|\hat{s}=0)|$$

1012 Therefore, f_{class} is a minimax estimator and the maximal ΔDP of BFtS is minimum among all
 1013 estimators of s .
 1014

\square

1015 At the global minima of θ_{class} , $|p(\hat{y}|\hat{s}=1) - p(\hat{y}|\hat{s}=0)|$ will be minimum. Its minimum value is 0.
 1016 Therefore, $p(\mathbf{h}|\hat{s}=1) - p(\mathbf{h}|\hat{s}=0) = 0$. The optimal θ_{class}^* achieves demographic parity for the
 1017 worst case.
 1018

1026 COROLLARY 1
10271028 *Proof.* If s' is a separate imputation independent of f_{class} and f_{bias} , then the min max game according
1029 to Dai & Wang (2021) is the following:
1030

1031
1032
$$\min_{\theta_{class}} \max_{\theta_{bias}} \mathbb{E}_{\mathbf{h} \sim p(\mathbf{h}|s'=1)} [\log f_{bias}(\mathbf{h})]$$

1033
$$+ \mathbb{E}_{\mathbf{h} \sim p(\mathbf{h}|s'=0)} [\log(1 - f_{bias}(\mathbf{h}))].$$

1034

1035 With optimal θ_{bias}^* , the optimization problem simplifies to-
1036

1037
$$\min_{\theta_{class}} -\log 4 + JS(p(\mathbf{h}|s'=1); p(\mathbf{h}|s'=0)).$$

1038 With independent imputation s' , the adversary f_{bias} tries to approximate the lower bound of Jensen
1039 Shannon Divergence (Weng, 2019). In BFtS, the adversarial imputation f_{imp} tries to approximate the
1040 upper bound of the JS divergence, and the classifier f_{class} tries to minimize the upper bound on the
1041 JS divergence provided by the adversarial imputation (see Proposition 1). Therefore,
1042

1043
$$JS((p(\mathbf{h}|s'=1); p(\mathbf{h}|s'=0))) \leq JS(p(\mathbf{h}|\hat{s}=1); p(\mathbf{h}|\hat{s}=0)).$$

□
1044
10451046 CONVERGENCE OF ADVERSARIAL LEARNING FOR THREE PLAYERS VS TWO PLAYERS WITH
1047 INDEPENDENT IMPUTATION
10481049 Let us consider a scenario when the independent missing sensitive value imputation (Dai & Wang,
1050 2021) fails to converge. There are three possible reasons for the convergence to fail:
10511052 1. s' is always 1
1053 2. s' is always 0
1054 3. s' is uniform, i.e. $p(\mathbf{h}|s'=1) = p(\mathbf{h}|s'=0)$ 1055 In scenario 1 and 2 the supports of $p(\mathbf{h}|s'=1)$ and $p(\mathbf{h}|s'=0)$ are disjoint. According to (Dai &
1056 Wang, 2021), the optimization for the classifier with an optimal adversary is
1057

1058
$$\min_{\theta_{class}} -\log 4 + 2JS(p(\mathbf{h}|s'=1); p(\mathbf{h}|s'=0))$$

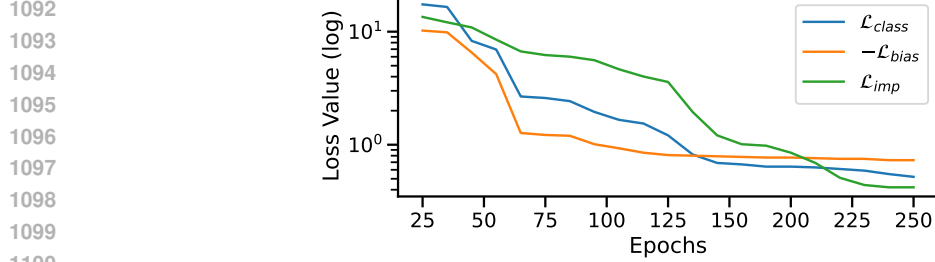
1059

1060 As the supports of $p(\mathbf{h}|s'=1)$ and $p(\mathbf{h}|s'=0)$ are disjoint, $JS(p(\mathbf{h}|s'=1); p(\mathbf{h}|s'=0))$ is
1061 always 0. The gradient of the JS divergence vanishes, and the classifier gets no useful gradient
1062 information—it will minimize a constant function. This results in extremely slow training of the node
1063 classifier, and it may not converge.1064 In scenario 3, \hat{s} is uniform. Therefore, $p(\mathbf{h}|s'=1)$ will be equal to $p(\mathbf{h}|s'=0)$ which results in
1065 $JS(p(\mathbf{h}|s'=1); p(\mathbf{h}|s'=0))$ being equal to 0. Moreover, the classifier may assign all training
1066 samples to a single class and yet have an adversary that may not be able to distinguish the sensitive
1067 attributes of the samples as \hat{s} is random. If the classifier assigns all samples to the majority class, it
1068 will achieve low classification loss \mathcal{L}_{class} along with minimum \mathcal{L}_{bias} . The training of the classifier
1069 may get stuck in this local minima (see Eq. 4). This phenomenon is similar to the mode collapse of
1070 GANs (Thanh-Tung & Tran, 2020).1071 Based on Corollary 1, our approach is more robust to the convergence issues described above.
10721073 TRAINING ALGORITHM
10741075 Algorithm 1 is a high-level description of the key steps applied for training BFtS. It receives the graph
1076 \mathcal{G} , labels y , labeled nodes \mathcal{V}_L , nodes with observed sensitive attributes \mathcal{V}_S and hyperparameters, α
1077 and β as inputs and outputs the GNN classifier f_{class} , sensitive attribute predictor, f_{bias} and missing
1078 data imputation GNN f_{imp} . We first estimate \hat{s} and then fix θ_{class} and θ_{bias} to update θ_{imp} . Then
1079 we update θ_{bias} with Eq. 5. After that, we fix θ_{bias} and θ_{imp} and update θ_{class} with Eq. 4 and repeat
these steps until convergence.

1080 **Algorithm 1** Training BFtS
1081 **Input:** $\mathcal{G}; y; \mathcal{V}_L; \mathcal{V}_S; \alpha, \beta$
1082 **Output:** $f_{class}, f_{bias}, f_{imp}$
1083 1: **repeat**
1084 2: Get the estimated sensitive attributes \hat{s}_i with f_{imp}
1085 3: Fix θ_{class} and θ_{bias} and update θ_{imp} using Eq. 6
1086 4: Update θ_{bias} using Eq. 5
1087 5: Fix θ_{imp} and θ_{bias} and update θ_{class} using Eq. 4
1088 6: **until** converge
1089

1090

1091



1092

1093

1094

1095

1096

1097

1098

1099

1100

Figure 6: Convergence of \mathcal{L}_{class} , \mathcal{L}_{bias} and \mathcal{L}_{imp} . All three losses converge smoothly, confirming theoretical stability.

1101

1102

1103

1104

1105

COMPLEXITY ANALYSIS

1106

1107

1108

BFtS model consists of two GNNs and one DNN. If we consider GCN for training the GNN, the time complexity is $\mathcal{O}(L|V|F^2 + L|E|F)$, and space complexity is $\mathcal{O}(LE + LF^2 + L|V|F)$, where L is the number of layers and F is the nodes in each layer (We assume that the number of nodes in each layer is the same) (Blakely et al., 2021). The complexity is polynomial, and therefore, BFtS is scalable. The complexity of FairGNN (Dai & Wang, 2021) is the same as the complexity of BFtS. FairGNN makes an additional forward pass to the trained sensitive attribute imputation network. Therefore, the empirical running time of FairGNN is higher than the one for BFtS, as shown in the next section.

1109

1110

1111

1112

1113

1114

1115

1116

1117

RUNNING TIME

1118

1119

1120

1121

1122

1123

Table 2 shows that Debias has the lowest runtime but performs the worst in fairness (See Fig. 4 and 5). BFtS had the second-lowest runtime. While the 3-player network adds complexity, it removes the requirement of training a separate imputation method (as for other benchmarks). Figure 6 presents

1124

1125

1126

1127

1128

1129

1130

1131

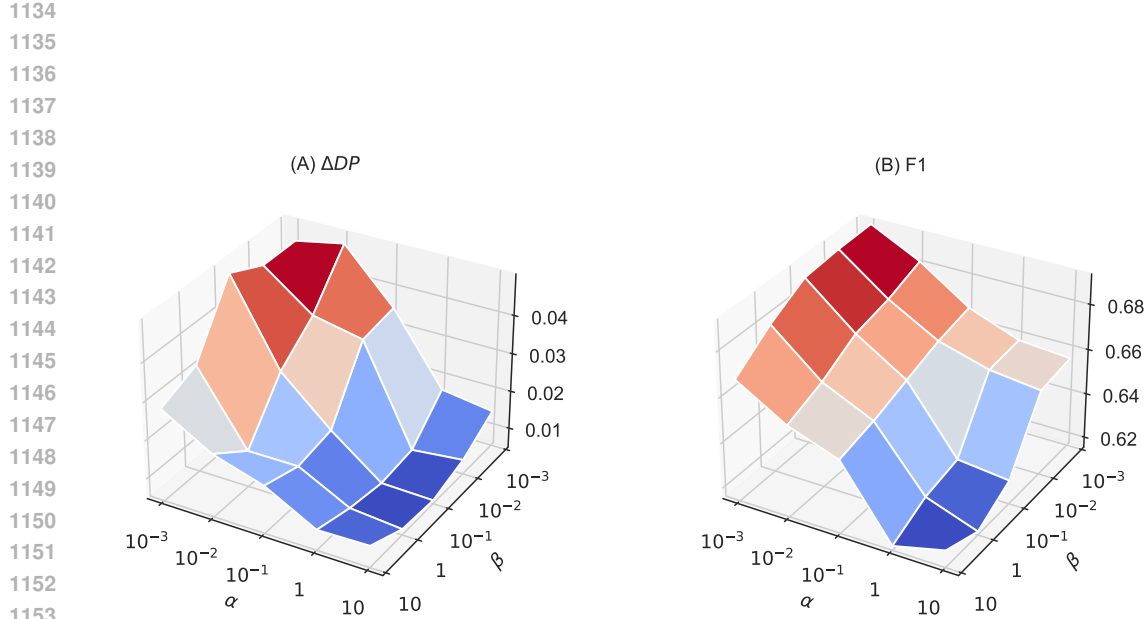
1132

1133

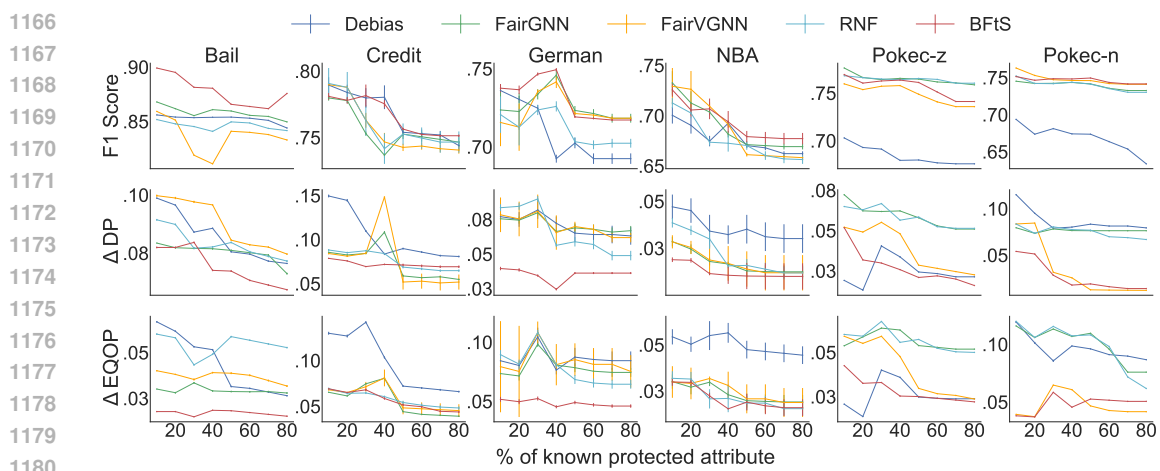
	German	Credit	Bail	NBA	pokec-z	pokec-n
Debias	21.74	110.99	170.95	14.85	650.67	647.62
FairGNN	31.43	229.41	340.48	29.12	1356.57	1234.62
FairVGNN	212.64	10557.79	2554.72	234.57	15956.62	15632.75
RNF	136.67	432.31	655.54	138.31	1945.58	2012.13
FairSIN	615.74	15142.25	2884.34	342.14	20565.13	20456.34
BFtS	28.91	168.88	242.88	22.34	942.35	956.42

Table 2: Running time (secs) of different methods

the convergence behavior of \mathcal{L}_{class} , \mathcal{L}_{bias} and \mathcal{L}_{imp} across training epochs on the NBA dataset.



1154
1155 Figure 7: Sensitivity analysis of α and β . BFtS is more sensitive to α than β . These parameters can
1156 be optimized using automated techniques, such as grid search.



1180
1181
1182 Figure 8: Performance of the models on different datasets for varying amounts of observed data \mathcal{V}_S .
1183 In the majority of the settings, our approach (BFtS) achieves a better fairness \times accuracy trade-off
1184 than the baselines.
1185
1186
1187

		VANILLA	DEBIAS	FairGNN	RNF	FairVGNN	FairSIN	BFtS (Ours)
1188	BAIL	AVPR (\uparrow)	0.86 \pm 0.00	0.81 \pm 0.00	0.82 \pm 0.00	0.81 \pm 0.00	0.80 \pm 0.00	0.81 \pm 0.00 0.83\pm0.00
1189		<i>F1 score</i> (\uparrow)	0.88 \pm 0.00	0.85\pm0.00	0.84 \pm 0.00	0.84 \pm 0.01	0.84 \pm 0.00	0.84 \pm 0.00 0.85\pm0.00
1190		$\% \Delta DP$ (\downarrow)	19.10 \pm 0.03	8.78 \pm 0.02	7.9 \pm 0.03	8.50 \pm 0.04	9.81 \pm 0.09	8.64 \pm 0.20 6.70\pm0.03
1191		$\% \Delta EQOP$ (\downarrow)	14.20 \pm 0.04	7.50 \pm 0.03	4.10 \pm 0.04	4.70 \pm 0.05	4.79 \pm 0.06	3.92 \pm 0.09 2.70\pm0.01
1192		$\% \Delta EQODDs$ (\downarrow)	11.49 \pm 0.08	8.61 \pm 0.02	5.28 \pm 0.08	3.42 \pm 0.07	5.01 \pm 0.02	4.96 \pm 0.01 2.81\pm0.02
1193	CREDIT	AVPR (\uparrow)	0.85 \pm 0.00	0.82 \pm 0.00	0.83\pm0.00	0.81 \pm 0.00	0.81 \pm 0.02	0.81 \pm 0.02 0.83\pm0.00
1194		<i>F1 score</i> (\uparrow)	0.79 \pm 0.00	0.73 \pm 0.00	0.76\pm0.00	0.75 \pm 0.01	0.73 \pm 0.00	0.75 \pm 0.00 0.76\pm0.00
1195		$\% \Delta DP$ (\downarrow)	12.10 \pm 0.10	8.80 \pm 0.20	5.60 \pm 0.08	5.30 \pm 0.09	7.77 \pm 0.25	5.21\pm0.12 5.40 \pm 0.02
1196		$\% \Delta EQOP$ (\downarrow)	14.50 \pm 0.10	9.20 \pm 0.10	5.90 \pm 0.10	5.10 \pm 0.00	5.56 \pm 0.21	4.95 \pm 0.13 4.50\pm0.01
1197		$\% \Delta EQODDs$ (\downarrow)	12.30 \pm 0.20	10.10 \pm 0.20	6.03 \pm 0.09	5.20 \pm 0.03	5.98 \pm 0.24	5.30 \pm 0.11 4.85\pm0.02
1198	GERMAN	AVPR (\uparrow)	0.75 \pm 0.00	0.72 \pm 0.00	0.73 \pm 0.00	0.72 \pm 0.01	0.70 \pm 0.01	0.73 \pm 0.00 0.74\pm0.00
1199		<i>F1 score</i> (\uparrow)	0.78 \pm 0.01	0.73 \pm 0.00	0.73 \pm 0.00	0.72 \pm 0.01	0.72 \pm 0.00	0.72 \pm 0.00 0.74\pm0.00
1200		$\% \Delta DP$ (\downarrow)	8.30 \pm 0.10	5.02 \pm 0.20	5.70 \pm 0.30	4.20 \pm 0.00	4.37 \pm 3.06	4.05 \pm 0.08 2.74\pm0.02
1201		$\% \Delta EQOP$ (\downarrow)	7.40 \pm 0.08	6.24 \pm 0.20	5.70 \pm 0.20	5.90 \pm 0.01	3.63 \pm 3.03	4.2 \pm 0.13 1.70\pm0.04
1202		$\% \Delta EQODDs$ (\downarrow)	7.78 \pm 0.01	6.91 \pm 0.30	5.91 \pm 0.08	6.26 \pm 0.08	3.75 \pm 1.13	5.01 \pm 0.08 2.14\pm0.03
1203	NBA	AVPR (\uparrow)	0.76 \pm 0.00	0.73 \pm 0.00	0.73 \pm 0.00	0.73 \pm 0.00	0.73 \pm 0.01	0.74\pm0.00
1204		<i>F1 score</i> (\uparrow)	0.73 \pm 0.00	0.67 \pm 0.00	0.70 \pm 0.00	0.69 \pm 0.00	0.69 \pm 0.05	0.70 \pm 0.02 0.71\pm0.00
1205		$\% \Delta DP$ (\downarrow)	13.10 \pm 0.02	6.40 \pm 0.04	1.20 \pm 0.03	1.50 \pm 0.05	2.39 \pm 1.2	1.5 \pm 0.21 1.10\pm0.04
1206		$\% \Delta EQOP$ (\downarrow)	11.50 \pm 0.02	5.50 \pm 0.02	5.30 \pm 0.00	3.10 \pm 0.03	4.19 \pm 2.1	3.9 \pm 0.07 2.70\pm0.01
1207		$\% \Delta EQODDs$ (\downarrow)	12.10 \pm 0.3	8.51 \pm 0.2	4.23 \pm 0.10	4.92 \pm 0.03	5.62 \pm 0.91	5.12 \pm 0.02 2.90\pm0.05
1208	POKEC-Z	AVPR (\uparrow)	0.76 \pm 0.00	0.72 \pm 0.00	0.72 \pm 0.00	0.73\pm0.00	0.72 \pm 0.07	0.71 \pm 0.05 0.73\pm0.00
1209		<i>F1 score</i> (\uparrow)	0.73 \pm 0.00	0.69 \pm 0.00	0.70 \pm 0.00	0.69 \pm 0.00	0.68 \pm 0.01	0.71\pm0.03 0.71 \pm 0.00
1210		$\% \Delta DP$ (\downarrow)	12.10 \pm 0.01	7.40 \pm 0.02	5.20 \pm 0.01	5.51 \pm 0.04	5.69 \pm 1.1	5.98 \pm 1.06 4.10\pm0.04
1211		$\% \Delta EQOP$ (\downarrow)	16.50 \pm 0.01	8.50 \pm 0.06	3.30 \pm 0.00	2.10 \pm 0.03	4.19 \pm 1.9	2.1 \pm 1.09 1.70\pm0.03
1212		$\% \Delta EQODDs$ (\downarrow)	13.10 \pm 0.04	7.59 \pm 0.02	3.18 \pm 0.08	2.81 \pm 0.04	5.09 \pm 1.02	2.56 \pm 0.57 1.91\pm0.04
1213	POKEC-N	AVPR (\uparrow)	0.74 \pm 0.00	0.71 \pm 0.00	0.72\pm0.00	0.72\pm0.00	0.70 \pm 0.08	0.71 \pm 0.02 0.72\pm0.00
1214		<i>F1 score</i> (\uparrow)	0.75 \pm 0.00	0.70 \pm 0.00	0.71 \pm 0.00	0.71 \pm 0.00	0.70 \pm 0.03	0.72 \pm 0.04 0.73\pm0.00
1215		$\% \Delta DP$ (\downarrow)	11.10 \pm 0.02	5.40 \pm 0.01	2.10 \pm 0.01	2.50 \pm 0.01	2.39 \pm 1.7	2.12 \pm 0.98 1.89\pm0.02
1216		$\% \Delta EQOP$ (\downarrow)	10.50 \pm 0.01	5.50 \pm 0.02	3.10 \pm 0.00	2.90 \pm 0.01	3.19 \pm 2.2	2.1 \pm 0.85 1.80\pm0.01
1217		$\% \Delta EQODDs$ (\downarrow)	11.56 \pm 0.02	6.15 \pm 0.03	4.81 \pm 0.04	3.04 \pm 0.02	4.51 \pm 2.13	3.49 \pm 0.05 2.05\pm0.04

Table 3: AVPR, F1 score, $\% \Delta DP$, $\% \Delta EQOP$, and $\% \Delta EQODDs$ of different methods. For the BAIL, and NBA dataset, we outperform all baselines in terms of accuracy and fairness. For other datasets, we improve fairness while slightly sacrificing accuracy.

1229
1230
1231
1232
1233
1234
1235
1236
1237
1238
1239
1240
1241

		VANILLA	DEBIAS	FAIRGNN	RNF	FairVGNN	FairSIN	BFtS (Ours)
1242 1243 1244 1245 1246	BAIL	AVPR (\uparrow)	0.88 \pm 0.00	0.81 \pm 0.00	0.81 \pm 0.00	0.82 \pm 0.00	0.82 \pm 0.01	0.83 \pm 0.01 0.84\pm0.00
		$F1$ (\uparrow)	0.71 \pm 0.00	0.59 \pm 0.00	0.68 \pm 0.00	0.62 \pm 0.003	0.66 \pm 0.01	0.69 \pm 0.02 0.70\pm0.00
		$\% \Delta DP$ (\downarrow)	11.10 \pm 0.04	12.70 \pm 0.04	8.20 \pm 0.03	9.80 \pm 0.05	8.48 \pm 0.51	8.31 \pm 0.03 7.9\pm0.04
		$\% \Delta EQOP$ (\downarrow)	8.90 \pm 0.01	6.50 \pm 0.06	4.30 \pm 0.03	5.90 \pm 0.01	5.88 \pm 0.08	3.96 \pm 0.21 2.80\pm0.02
		$\% \Delta EQODDs$ (\downarrow)	9.18 \pm 0.02	6.93 \pm 0.02	5.21 \pm 0.04	6.42 \pm 0.03	5.89 \pm 0.06	4.21 \pm 0.26 2.93\pm0.02
1247 1248 1249 1250 1251	CREDIT	AVPR (\uparrow)	0.79 \pm 0.00	0.73 \pm 0.00	0.75 \pm 0.00	0.75 \pm 0.01	0.76\pm0.00	0.74 \pm 0.00
		$F1$ (\uparrow)	0.71 \pm 0.00	0.68 \pm 0.00	0.69 \pm 0.00	0.71\pm0.00	0.70 \pm 0.00	0.70 \pm 0.00 0.71\pm0.00
		$\% \Delta DP$ (\downarrow)	14.20 \pm 0.02	9.10 \pm 0.02	8.02 \pm 0.05	6.40 \pm 0.04	6.70 \pm 0.05	5.01 \pm 0.20 4.20\pm0.02
		$\% \Delta EQOP$ (\downarrow)	18.30 \pm 0.20	15.12 \pm 0.08	12.15 \pm 0.10	10.95 \pm 0.06	9.75 \pm 0.09	9.31 \pm 0.09 8.60\pm0.04
		$\% \Delta EQODDs$ (\downarrow)	15.51 \pm 0.10	10.22 \pm 0.01	9.04 \pm 0.32	9.92 \pm 0.05	8.96 \pm 0.02	8.54 \pm 0.10 7.57\pm0.02
1252 1253 1254	GERMAN	AVPR (\uparrow)	0.73 \pm 0.00	0.70 \pm 0.00	0.71 \pm 0.00	0.72\pm0.00	0.71 \pm 0.00	0.70 \pm 0.00
		$F1$ (\uparrow)	0.74 \pm 0.00	0.71 \pm 0.00	0.70 \pm 0.00	0.72 \pm 0.01	0.71 \pm 0.00	0.71 \pm 0.01 0.72\pm0.00
		$\% \Delta DP$ (\downarrow)	9.80 \pm 0.07	6.12 \pm 0.06	6.70 \pm 0.10	7.10 \pm 0.00	6.01 \pm 0.06	5.01 \pm 0.02 4.1\pm0.04
		$\% \Delta EQOP$ (\downarrow)	10.80 \pm 0.04	6.70 \pm 0.10	5.80 \pm 0.04	6.10 \pm 0.06	5.20 \pm 0.07	4.13 \pm 0.09 3.90\pm0.04
		$\% \Delta EQODDs$ (\downarrow)	11.15 \pm 0.05	6.87 \pm 0.20	6.13 \pm 0.05	5.89 \pm 0.06	4.97 \pm 0.03	4.76 \pm 0.02 3.21\pm0.05
1255 1256 1257 1258 1259	NBA	AVPR (\uparrow)	0.74 \pm 0.00	0.70 \pm 0.00	0.71 \pm 0.00	0.72\pm0.00	0.71 \pm 0.00	0.70 \pm 0.00
		$F1$ (\uparrow)	0.79 \pm 0.00	0.75 \pm 0.00	0.75 \pm 0.00	0.75 \pm 0.01	0.74 \pm 0.08	0.76\pm0.00
		$\% \Delta DP$ (\downarrow)	7.60 \pm 0.03	4.20 \pm 0.03	2.30 \pm 0.01	3.10 \pm 0.04	2.10 \pm 0.04	3.19 \pm 0.10 2.01\pm0.01
		$\% \Delta EQOP$ (\downarrow)	11.20 \pm 0.03	5.40 \pm 0.04	3.30 \pm 0.01	3.30 \pm 0.01	3.12 \pm 0.05	2.91 \pm 0.05 2.10\pm0.01
		$\% \Delta EQODDs$ (\downarrow)	10.21 \pm 0.04	6.51 \pm 0.02	3.65 \pm 0.07	3.95 \pm 0.02	3.48 \pm 0.08	2.85 \pm 0.02 1.89\pm0.02
1260 1261 1262 1263 1264	POKEC-Z	AVPR (\uparrow)	0.78 \pm 0.00	0.73 \pm 0.00	0.74\pm0.00	0.73 \pm 0.00	0.73 \pm 0.07	0.74 \pm 0.05 0.74\pm0.00
		$F1$ (\uparrow)	0.75 \pm 0.00	0.71 \pm 0.00	0.72 \pm 0.00	0.72 \pm 0.00	0.73 \pm 0.01	0.73 \pm 0.03 0.74\pm0.00
		$\% \Delta DP$ (\downarrow)	10.19 \pm 0.07	8.21 \pm 0.08	5.98 \pm 0.07	5.18 \pm 0.08	5.79 \pm 1.08	4.98 \pm 2.01 3.90\pm0.05
		$\% \Delta EQOP$ (\downarrow)	12.13 \pm 0.01	6.85 \pm 0.02	2.98 \pm 0.02	2.38 \pm 0.07	3.15 \pm 2.01	2.90 \pm 1.07 1.98\pm0.01
		$\% \Delta EQODDs$ (\downarrow)	13.13 \pm 0.02	6.93 \pm 0.06	3.15 \pm 0.07	2.95 \pm 0.03	2.65 \pm 1.01	2.13 \pm 0.97 1.79\pm0.02
1265 1266 1267 1268 1269	POKEC-N	AVPR (\uparrow)	0.75 \pm 0.00	0.72 \pm 0.00	0.72 \pm 0.00	0.72 \pm 0.00	0.71 \pm 0.08	0.72 \pm 0.04 0.73\pm0.00
		$F1$ (\uparrow)	0.78 \pm 0.00	0.75 \pm 0.00	0.75 \pm 0.00	0.74 \pm 0.00	0.74 \pm 0.02	0.75 \pm 0.01 0.76\pm0.00
		$\% \Delta DP$ (\downarrow)	14.10 \pm 0.01	6.51 \pm 0.02	3.40 \pm 0.02	4.12 \pm 0.02	2.98 \pm 1.9	2.75 \pm 1.2 1.89\pm0.02
		$\% \Delta EQOP$ (\downarrow)	12.50 \pm 0.07	5.50 \pm 0.02	3.10 \pm 0.00	2.90 \pm 0.01	3.19 \pm 2.2	2.1 \pm 0.85 1.80\pm0.01
		$\% \Delta EQODDs$ (\downarrow)	13.57 \pm 0.03	5.91 \pm 0.04	3.70 \pm 0.01	3.20 \pm 0.01	2.91 \pm 1.03	2.43 \pm 0.06 1.71\pm0.05

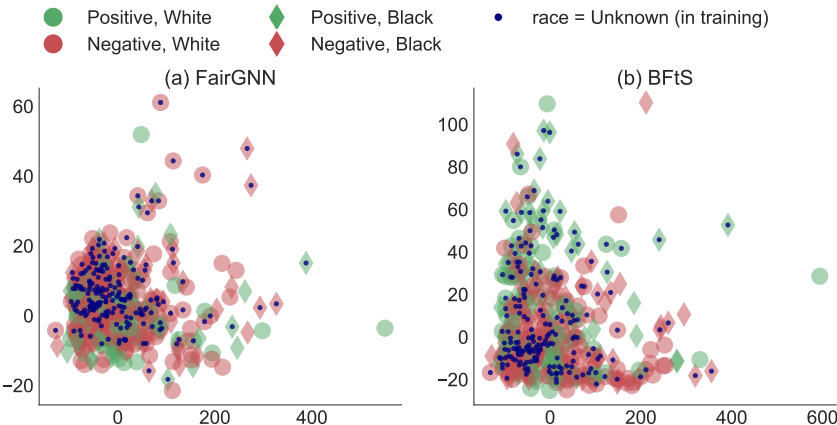
Table 4: AVPR, F1, $\% \Delta DP$, $\% \Delta EQOP$, and $\% \Delta EQODDs$ of different methods. GAT is the GNN architecture for all models. For the BAIL dataset, our model outperforms every other baseline in terms of fairness and accuracy. For the GERMAN, NBA and CREDIT datasets, we perform more fairly but less accurately.

1284
1285
1286
1287
1288
1289
1290
1291
1292
1293
1294
1295

1296 IMPUTATION ACCURACY
1297

1298 Table 5 shows the imputation accuracy of the methods. We exclude results for Debias, which is
1299 based only on the sensitive information available, and for FairVGNN and FairSIN, as they are
1300 identical to FairGNN (same imputation method). The results show that BFtS imputation outperforms
1301 independent imputation methods. BFtS worst-case imputation based on the LDAM loss outperforms
1302 the alternatives in terms of accuracy. This is due to the adversarial missingness process where
1303 low-degree nodes are selected to have missing values. Independent imputation methods are less
1304 effective in this adversarial setting.

	German	Credit	Bail	NBA	pokec-z	pokec-n
FairGNN	0.70	0.90	0.56	0.78	0.81	0.84
RNF	0.59	0.73	0.53	0.64	0.65	0.68
BFtS	0.72	0.94	0.63	0.78	0.83	0.87

1309 Table 5: Accuracy of missing sensitive imputation.
1310

1326 Figure 9: 2-D kernel PCA node representations for the BAIL dataset generated by the FairGNN and
1327 BFtS (our approach). We use different markers for nodes depending on their predicted class, sensitive
1328 attribute (race), and whether the sensitive attribute is missing. The results show that representations
1329 for nodes with missing values are more biased for FairGNN where they are concentrated in a negative
1330 class region. On the other hand, nodes with missing values are better spread over the space for BFtS
1331 representations. In BFtS, there are more ‘Race = Black’ nodes than in FairGNN that have missing
1332 sensitive values in training but are predicted to be positive.

1334 WORST-CASE FAIRNESS ACCURACY TRADE-OFF
1335

1336 As our proposed model operates under a worst-case fairness assumption, it may overestimate the
1337 bias in the complete data, as illustrated in Figure 2 using the BAIL dataset. This results in a trade-off
1338 between fairness and utility, which is governed by a hyperparameter β . Figures 10(a), (b), and (c)
1339 show the F1 score, $1 - \Delta DP$, and $1 - \Delta EQOP$, respectively, as β varies and with 30% of sensitive
1340 values observed. Here, F1 serves as the utility metric, while $1 - \Delta DP$ and $1 - \Delta EQOP$ quantify
1341 fairness. We compare our BFtS model against a fair adversarial model trained with complete sensitive
1342 information. By tuning β , we balance predictive utility and fairness under worst-case bias, achieving
1343 an effective trade-off.

1344 ADDITIONAL EXPERIMENTS
13451346 LARGE SCALE GRAPH DATASET
1347

1348 To verify the performance of BFtS on large-scale dataset, we generated a synthetic graph with 250k
1349 nodes and 100 features, as we were unable to identify a large-scale real-world graph dataset with

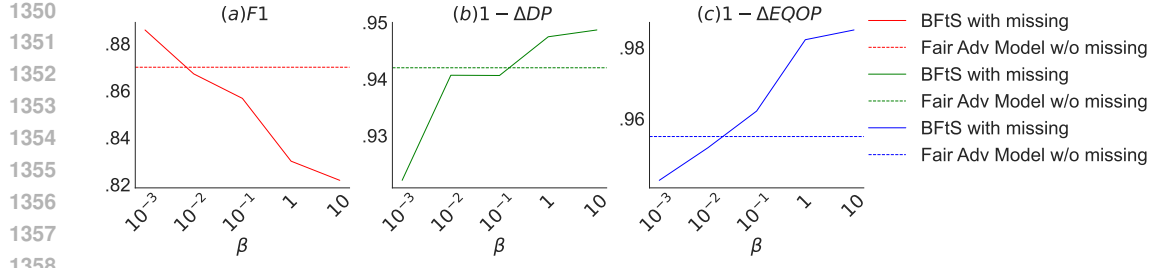


Figure 10: Fairness–utility trade-off of BFtS on the BAIL dataset as β varies, compared to a fair adversarial model trained with complete data. Lower β yields higher accuracy but lower fairness.

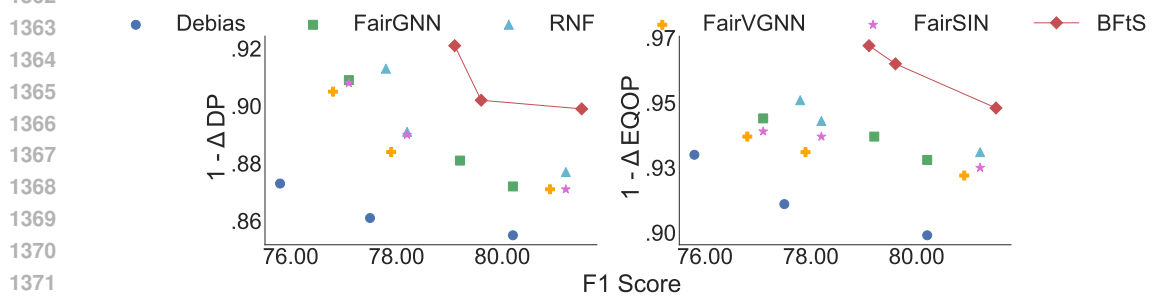


Figure 11: Fairness accuracy trade off for large scale graph dataset. BFtS achieves better fairness-accuracy trade-off

sensitive values. Following the setup in Figure 4 (with 150k nodes in the non-protected group and assortativity = 0.77). We compared BFtS against other baselines in Figure 11 across different hyperparameter settings. BFtS completed training in 85.4 minutes versus RNF’s (the strongest baseline in this scenario) 114.6 minutes.

AVERAGE PERFORMANCE WITH GCN AND GAT

Table 3 shows the average results for BAIL, CREDIT, GERMAN, and NBA datasets. In terms of accuracy and fairness, BFtS outperforms all baseline approaches for the BAIL and NBA datasets. We also outperform competitors on the CREDIT and GERMAN datasets in terms of fairness, with a slight AVPR loss. Although we lose some AVPR in the GERMAN and CREDIT datasets, we win in F1 and the AVPR loss is negligible when compared to the fairness benefit. Table 4 shows the average results for BAIL, CREDIT, GERMAN, and NBA datasets using GAT Velickovic et al. (2017) to train f_{class} and f_{imp} . In terms of accuracy and fairness, BFtS outperforms all baseline approaches for the BAIL dataset. We also outperform competitors on the CREDIT, GERMAN, and NBA datasets in terms of fairness with a slight AVPR loss. The AVPR loss is negligible when compared to the fairness benefit.

VISUALIZATION OF REPRESENTATIONS

Figure 9 shows kernel PCA node representations produced by FairGNN and BFtS using the BAIL dataset. We show the samples with missing "Race" with a navy dot in the middle and samples predicted as positive class and negative class in green and red, respectively. The representations generated by FairGNN are noticeably more biased than the ones generated by our approach. A higher number of "Race = Black" samples with missing sensitive values in training are predicted as positive by BFtS than for FairGNN. Moreover, BFtS spreads nodes with missing values more uniformly over the space. This illustrates how the missing value imputation of FairGNN underestimates the bias in the training data and, therefore, the model could not overcome the bias in the predictions.

1404	Method	MSE (\pm)	ΔDP (\pm)
1405	BFtS	0.71 ± 0.10	0.15 ± 0.02
1406	Vanilla	0.65 ± 0.10	0.21 ± 0.01

Table 6: Fair regression: MSE and Fairness (ΔDP) Comparison Between BFtS and Vanilla Models

1410		CROSS ENTROPY f_{imp}				LDAM f_{imp}			
		AVPR (\uparrow)	F1 (\uparrow)	$\% \Delta DP$ (\downarrow)	$\% \Delta EQOP$ (\downarrow)	AVPR(\uparrow)	F1(\uparrow)	$\% \Delta DP$ (\downarrow)	$\% \Delta EQOP$ (\downarrow)
1411	GERMAN	0.75 ± 0.00	0.73 ± 0.00	4.10 ± 0.05	3.70 ± 0.03	0.74 ± 0.00	0.74 ± 0.00	2.74 ± 0.02	1.7 ± 0.04
1412	CREDIT	0.83 ± 0.00	0.77 ± 0.01	5.55 ± 0.03	4.70 ± 0.05	0.83 ± 0.00	0.76 ± 0.00	5.4 ± 0.02	4.5 ± 0.01
1413	BAIL	0.85 ± 0.00	0.85 ± 0.00	7.10 ± 0.02	3.1 ± 0.06	0.83 ± 0.00	0.85 ± 0.00	6.70 ± 0.03	2.7 ± 0.01
1414	NBA	0.75 ± 0.00	0.72 ± 0.00	2.11 ± 0.03	3.5 ± 0.02	0.74 ± 0.00	0.71 ± 0.00	1.10 ± 0.04	2.70 ± 0.01
1415	SIMULATION	0.94 ± 0.00	0.96 ± 0.00	16.00 ± 0.03	8.00 ± 0.08	0.92 ± 0.00	0.96 ± 0.01	12.00 ± 0.03	5.10 ± 0.04

Table 7: Ablation study using LDAM loss and cross-entropy loss for f_{imp} . Using LDAM loss gives a better fairness and accuracy trade-off.

FAIR NODE REGRESSION

While fairness-aware node regression datasets are lacking, we created a synthetic node regression task (assortativity = 0.77) following our setup in Figure 5, with group-wise targets from $\mathcal{N}(0, 1)$ and $\mathcal{N}(2, 1)$. The Table 6 reports MSE and ΔDP (Berk et al., 2017) for regression.

ABLATION STUDY

To see the impact of α and β , we train BFtS on the GERMAN dataset with different values of α and β . We consider values between $[10^{-3}, 10^{-2}, 10^{-1}, 1, 10]$ for both α and β . Figure 7 shows the ΔDP and F1 of BFtS on the GERMAN dataset. α and β control the impact of the adversarial loss \mathcal{L}_A on the GNN classifier and the missing value imputation GNN, respectively. The figure shows that α has a larger impact than β on the fairness and accuracy of the model.

We also vary the amount of observed data \mathcal{V}_S and plot the results in Figure 8. We use 10%, 20%, ..., 80%, of training nodes as \mathcal{V}_S . For nearly all models, fairness increases and accuracy decreases with $|\mathcal{V}_S|$. With BFtS, both accuracy and bias often decline with the increase of \mathcal{V}_S . In the majority of the settings, our approach (BFtS) achieves a better fairness \times accuracy trade-off than the baselines.

To see the impact of LDAM loss, we train f_{imp} with cross-entropy loss and compare the performance with f_{imp} trained with LDAM loss in Table 7. Evidently, LDAM achieves a better trade-off between accuracy and fairness.